

XXIV International Baldin Seminar
on High Energy Physics Problems 2018

Highlights from the STAR experiment

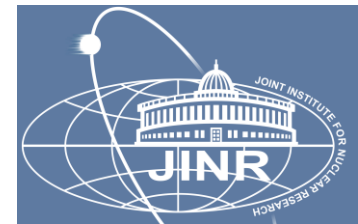


Alexey Aparin
For the STAR collaboration

Joint Institute for Nuclear Research



XXIV ISHEPP, September 17 -22, Dubna, Russia

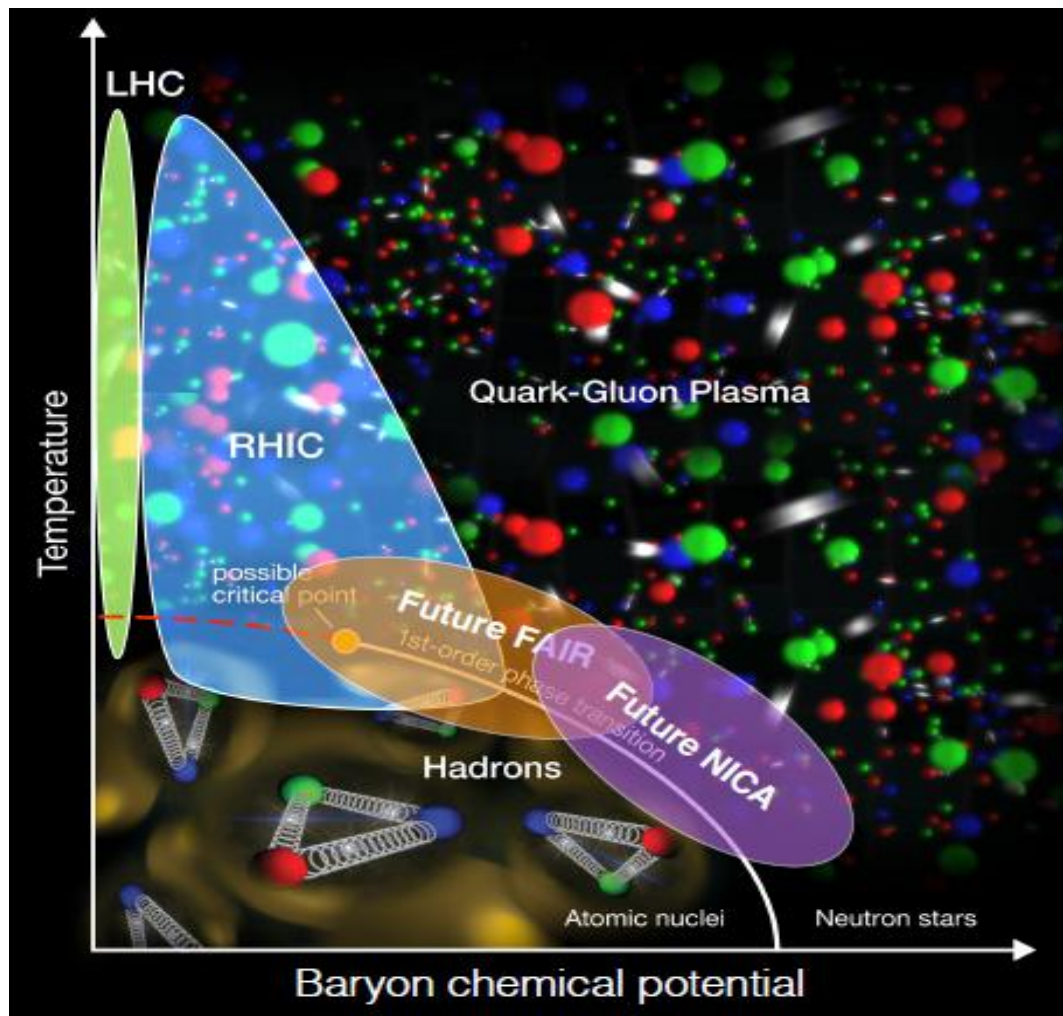




Outline

- Introduction
- Azimuthal anisotropy
- Heavy flavor
- Global polarization
- Femtoscopy
- Fixed target program
- Hypertriton
- STAR future program

Introduction



Picture from QM18 presentation by Chun Shen

RHIC Top Energy

$p+p$, $p+Al$, $p+Au$, $d+Au$, ^3He+Au ,
 $Cu+Cu$, $Cu+Au$, $Ru+Ru$, $Zr+Zr$,
 $Au+Au$, $U+U$ 200 GeV
QCD at high energy
density/temperature
Properties of QGP, EoS

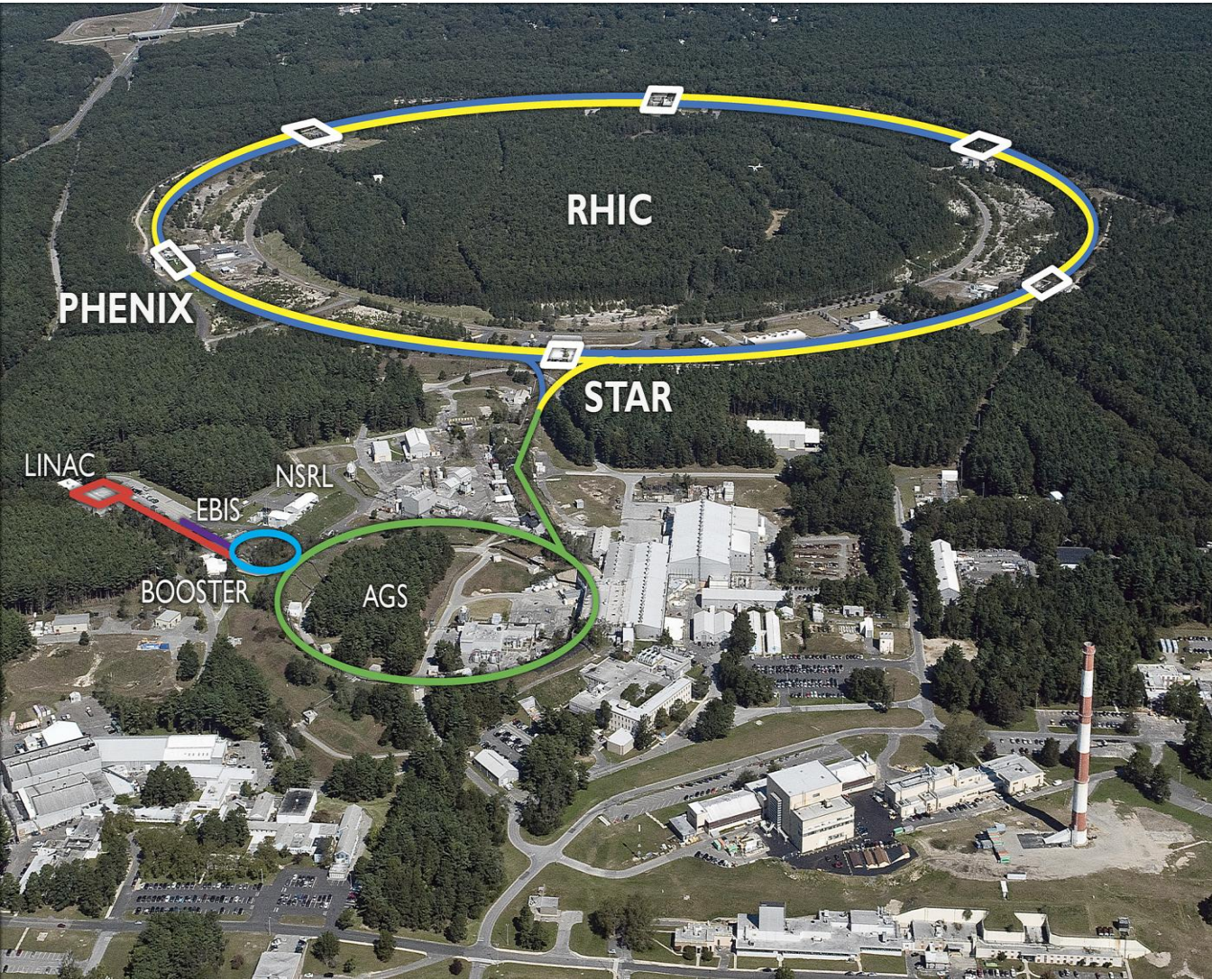
Beam Energy Scan

$Au+Au$ 7.7-62 GeV
QCD phase transition
Search for critical point
Turn-off of QGP signatures

Fixed-Target Program

$Au+Au$ 3.0-7.7 GeV
High baryon density regime
with 420-720 MeV

Relativistic Heavy Ion Collider



In operation since 1999

3.83 km circumference

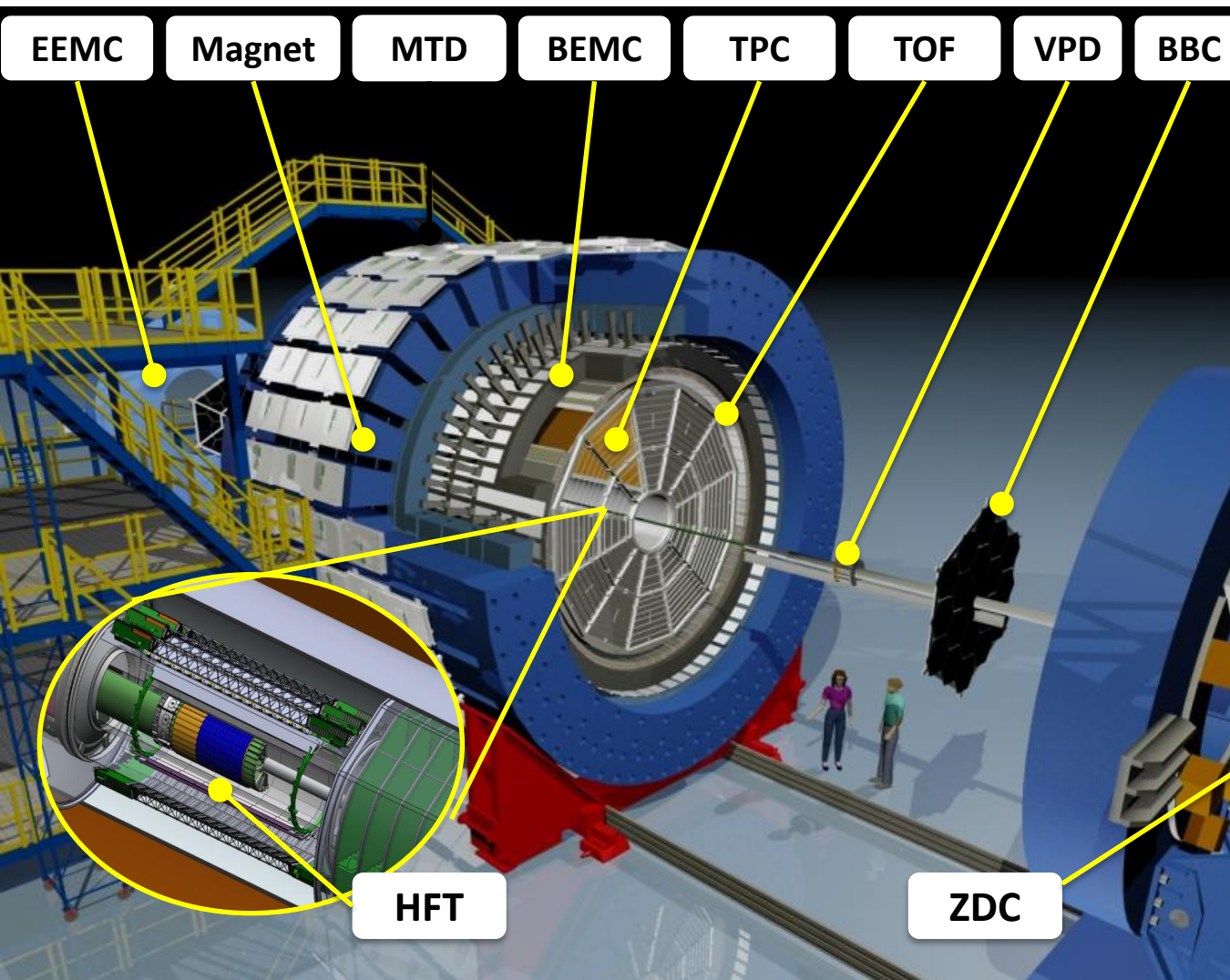
Suitable for p+p, p+A, A+A

Max colliding energy:
200 GeV for Au+Au
510 GeV for p+p

Tuned for exploring QCD matter and its phase boundary in different colliding systems (Au+Au, U+U, p+Al, Cu+Au, Zr+Zr, Ru+Ru)

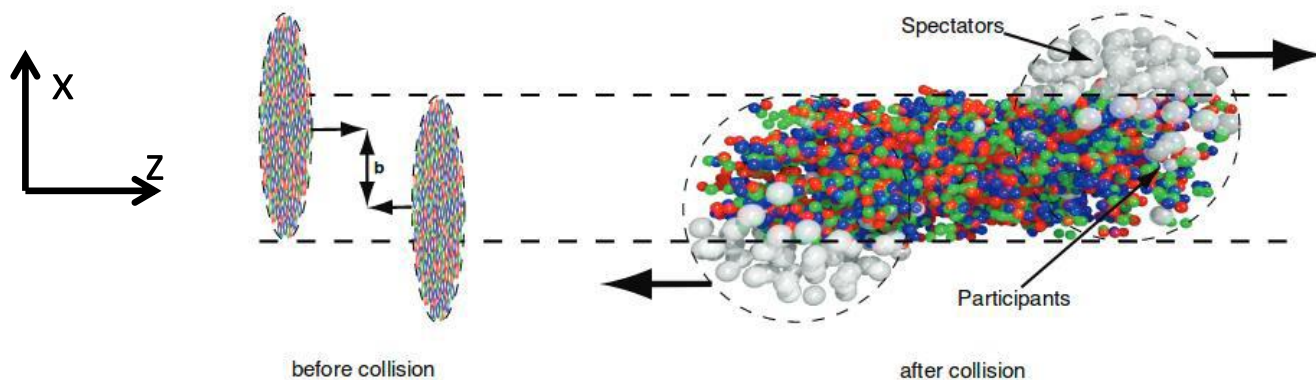
Spin physics on polarized proton-proton beam

STAR detector



- **Tracking and PID (full 2π)**
 - TPC: $|\eta| < 1$
 - TOF: $|\eta| < 1$
 - BEMC: $|\eta| < 1$
 - EEMC: $1 < \eta < 2$
 - HFT (2014-2016): $|\eta| < 1$
 - MTD (2014+): $|\eta| < 0.5$
- **MB Trigger and event plane reconstruction**
 - BBC: $3.3 < |\eta| < 5$
 - EPD(2018+): $2.1 < |\eta| < 5.1$
 - FMS: $2.5 < |\eta| < 4$
 - VPD: $4.2 < |\eta| < 5$
 - ZDC: $6.5 < |\eta| < 7.5$
- **On-going/future upgrades**
 - iTPC (2019+): $|\eta| < 1.5$
 - eTOF (2019+): $-1.6 < \eta < -1$
 - FCS (2021+): $2.5 < |\eta| < 4$
 - FTS (2021+): $2.5 < |\eta| < 4$

Azimuthal anisotropy in heavy ion collisions



$$E \frac{d^3 N}{dp^3} = \frac{1}{2\pi} \frac{d^2 N}{p_t dp_t dy} \left(1 + \sum_{n=1}^{\infty} 2v_n \cos[n(\varphi - \Psi_r)] \right)$$

Coordinate space anisotropy transforms to momentum space anisotropy

$v_1 = \langle p_x/p_t \rangle$ describes the sideward collective motion of particles within the reaction plane (x-z)

Probe of the softening of the EoS

- Strong softening consistent with the 1st order phase transition
- Weak softening is more likely due to crossover

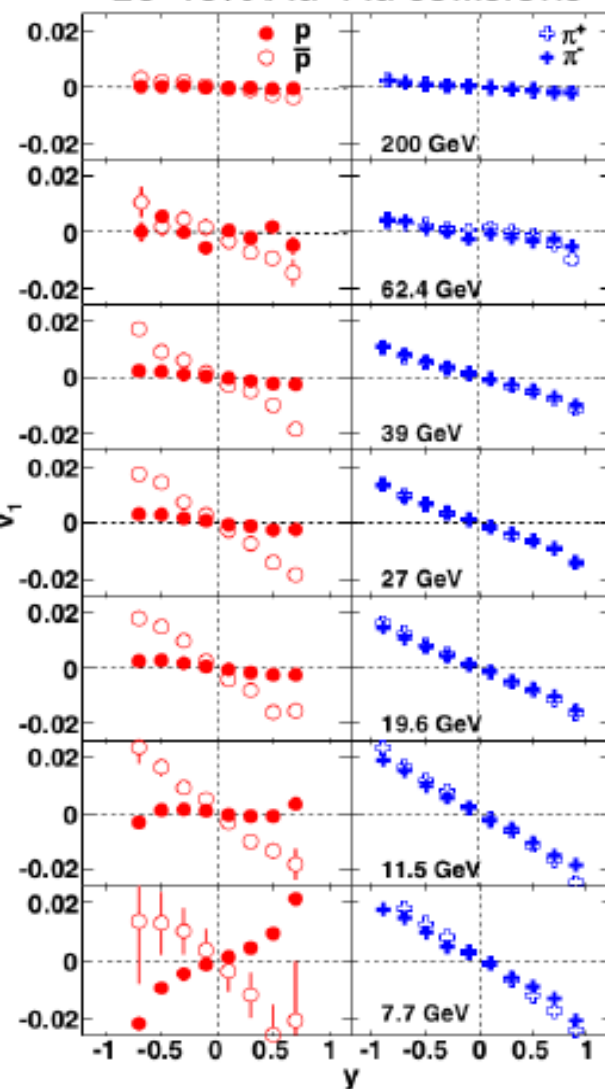
Voloshin, Zhang. Z. Phys. C 70 (1996) 665

Poskanzer, Voloshin. Phys Rev. C 58 (1998) 1671

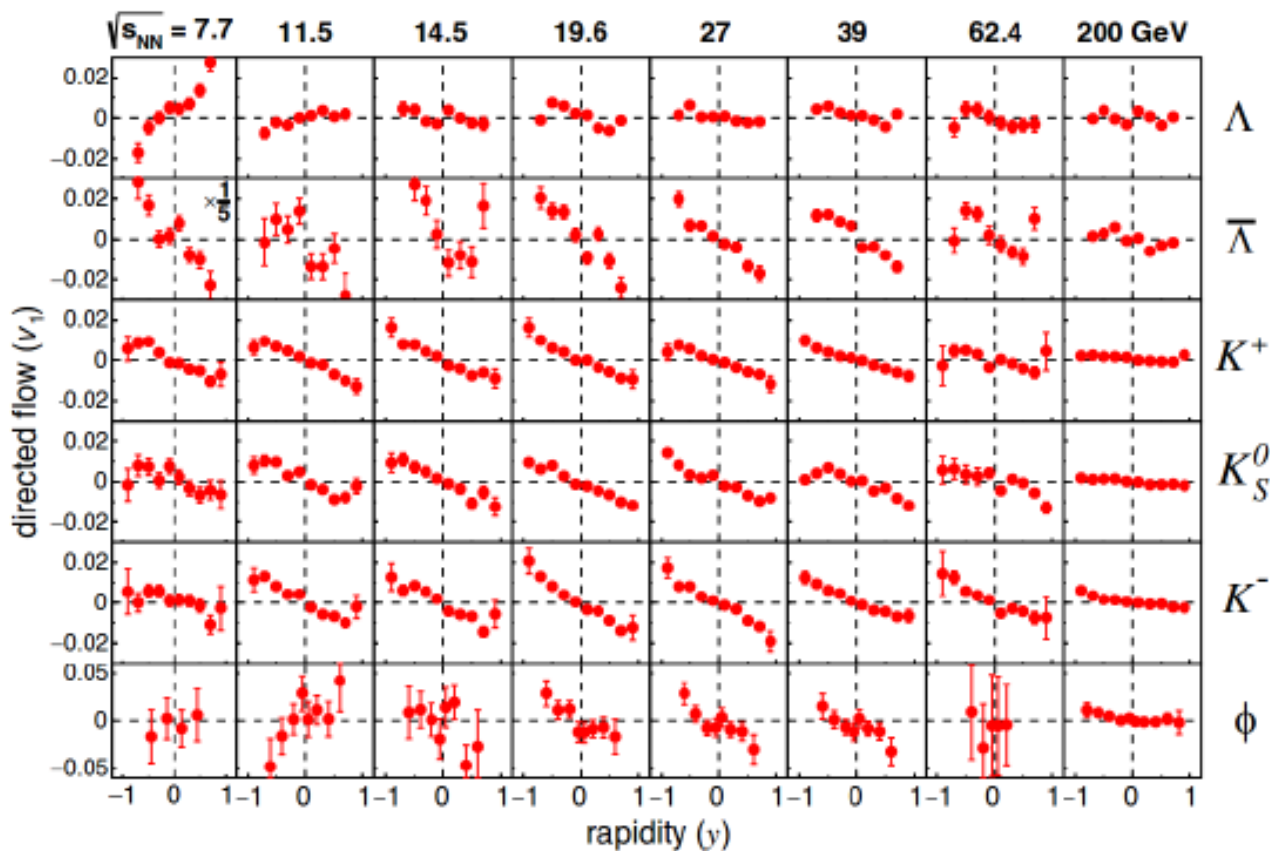
Directed flow with light flavors



10-40% Au+Au collisions



To extract v_1 slope, use linear fit over $|y| < 0.6$ for Φ and over $|y| < 0.8$ for all other species



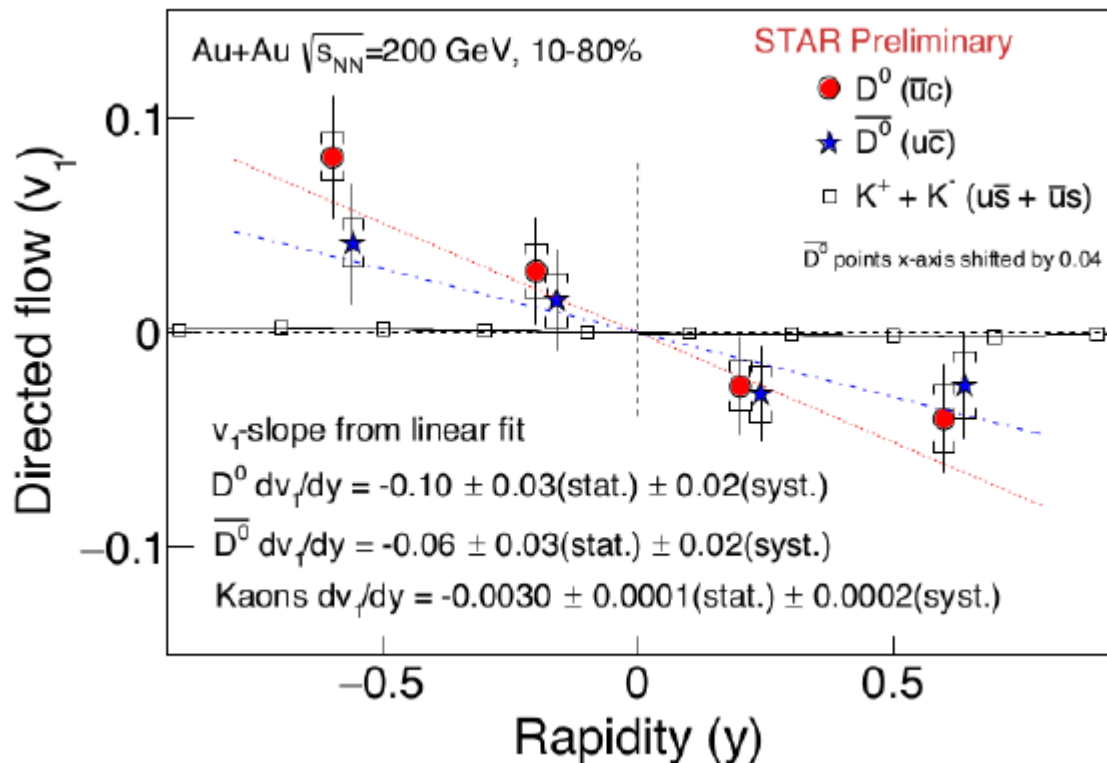
Phys. Rev. Lett. 112 (2014) 162301

Phys. Rev. Lett. 120 (2018) 062301

Directed flow of D^0



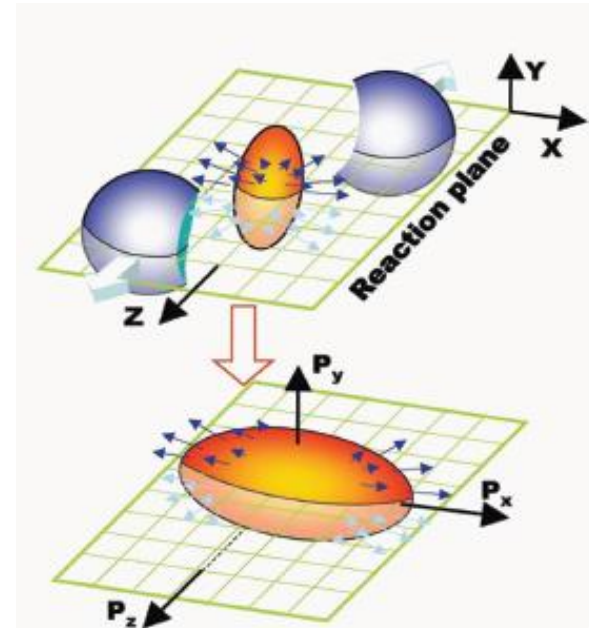
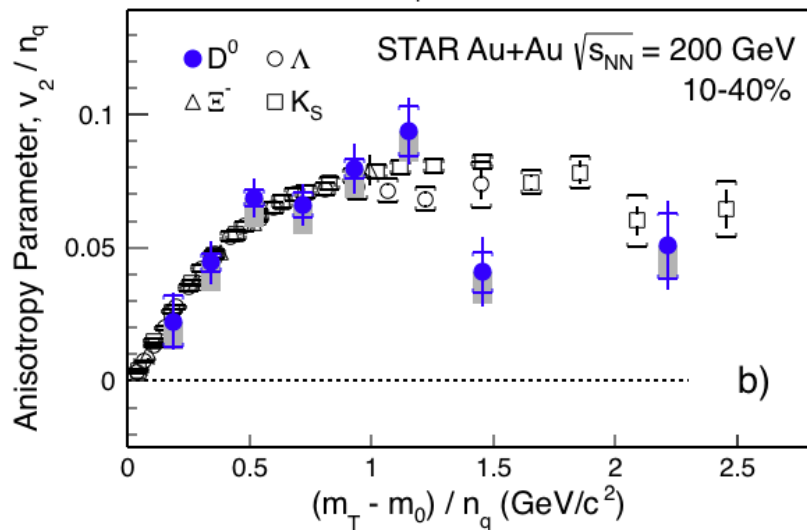
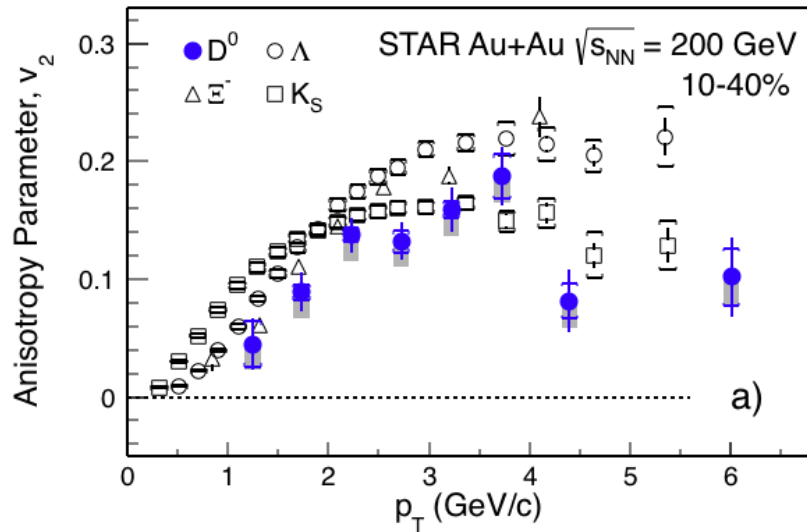
Non-zero v_1 for D^0 observed for the first time



Data from 2014+2016 Heavy Flavor Tracker (HFT)

$$D^0 + \bar{D}^0 dv_1 / dy = -0.081 \pm 0.021(stat.) \pm 0.017(syst.)$$

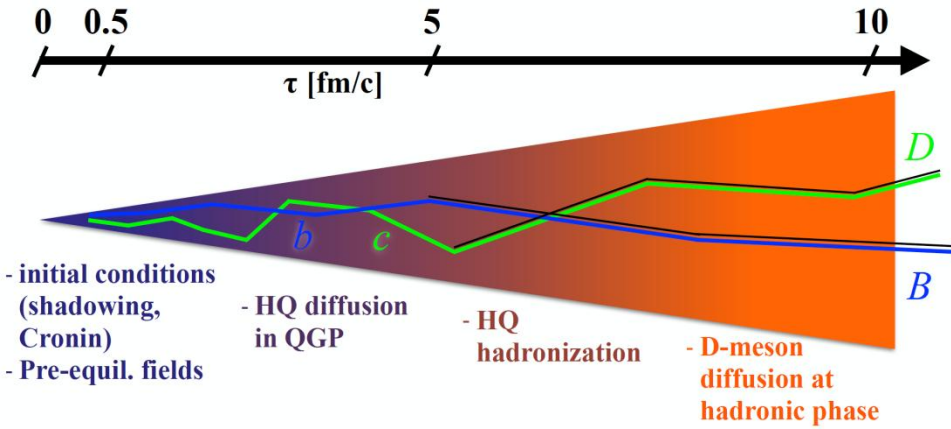
Elliptic flow of D^0



Charm quarks seem to follow NCQ-scaling behavior as light quarks
Charm quarks gain significant flow

Phys Rev. Lett. 118, 212301 (2017)

Nuclear modification and heavy flavor in medium



- initial conditions
(shadowing,
Cronin)
- Pre-equil. fields

- HQ diffusion
in QGP

- HQ
hadronization

- D-meson
diffusion at
hadronic phase

Partons interact with the medium and lose energy through e.g. gluon radiation

Quarks are expected to exhibit different radiative energy loss depending on their mass (D.Kharzeev et al. Phys Letter B. 519:1999)

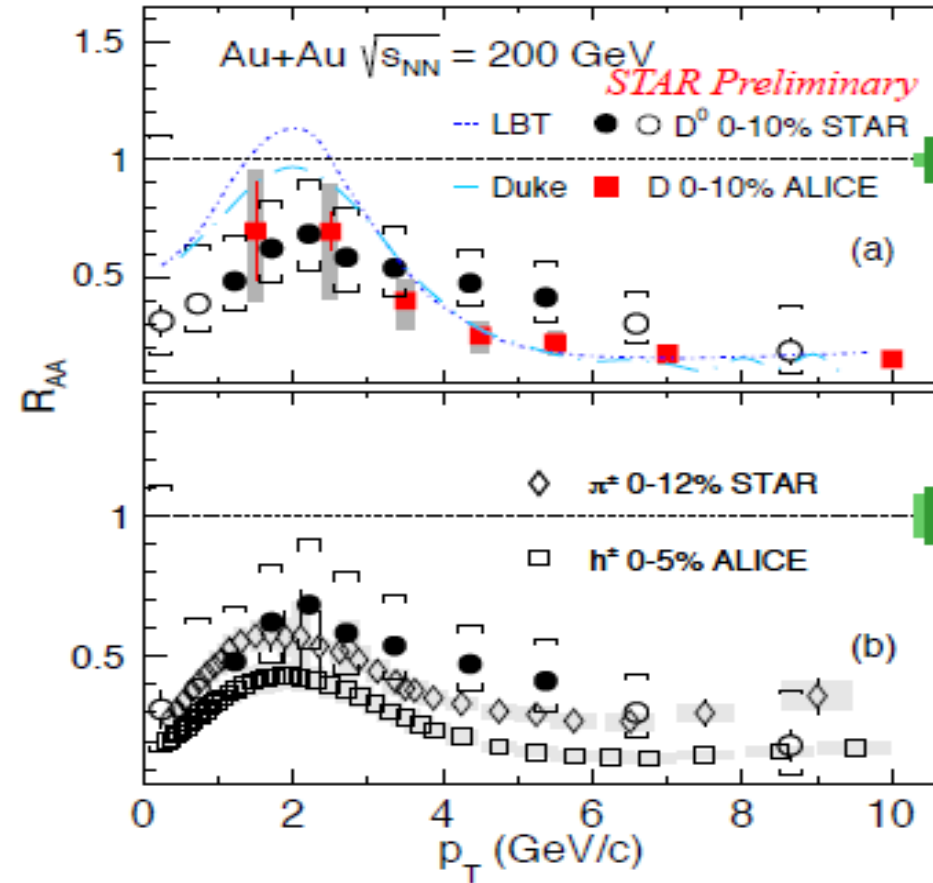
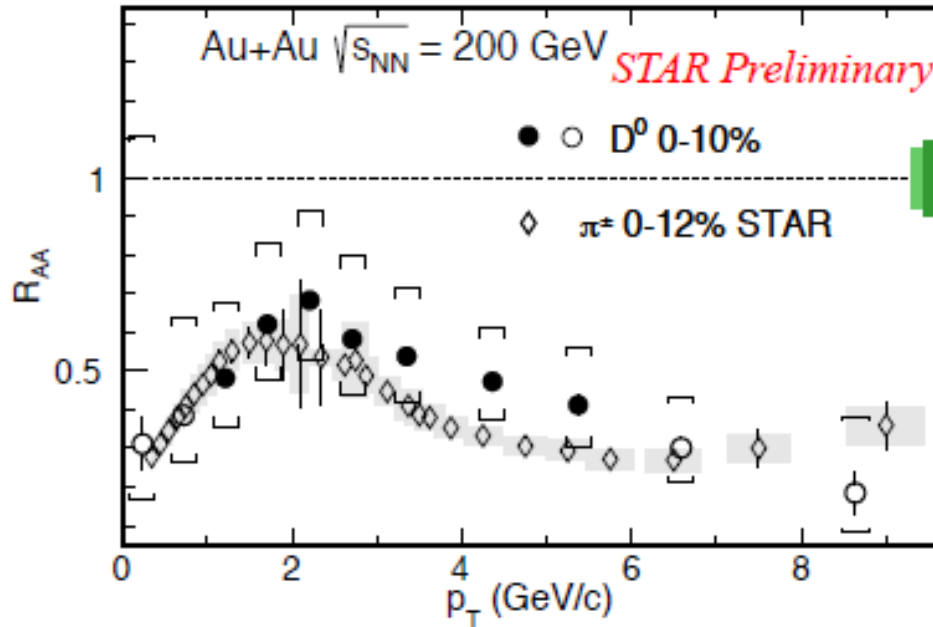
Nuclear Modification factor:

$$R_{AA}(p_t) = \frac{\sigma_{in}^{pp}}{\langle N_{coll}^{AA} \rangle} \cdot \frac{d^2 N_{AA} / dp_t d\eta}{d^2 \sigma_{pp} / dp_t d\eta}$$

Large collective flow and modification of yields for charm hadrons in A+A collisions

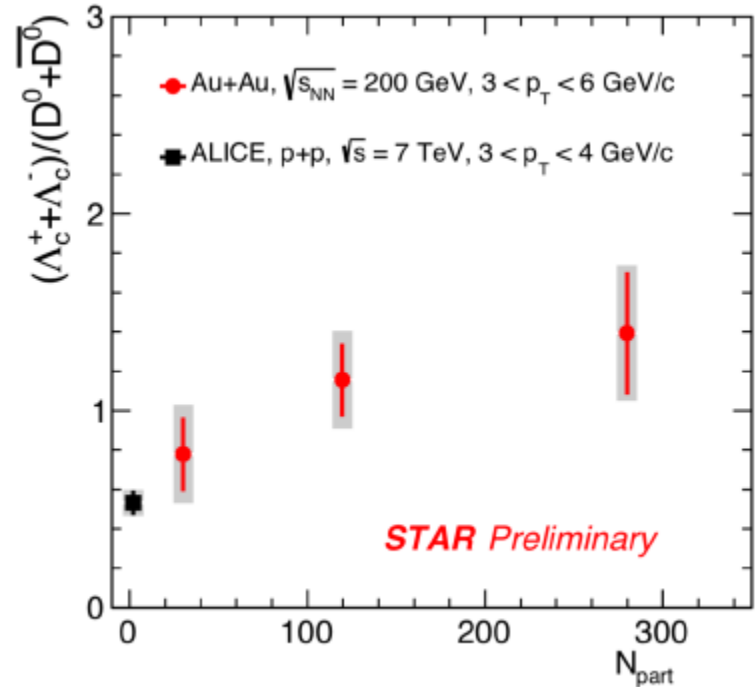
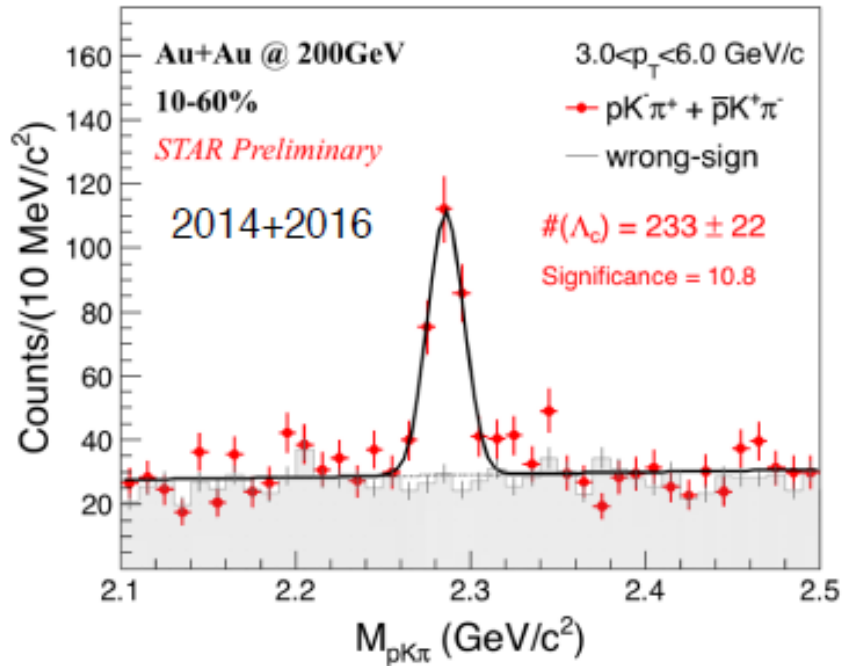
Understand heavy quark production, transport and hadronization in the presence of QGP

Nuclear modification factor for D^0



- R_{AA} in central events < 1 at all p_T
- Suppression at high p_T increases with centrality
- Similar to D-mesons at LHC and high- p_T pions at RHIC

Λ_c production at 200 GeV



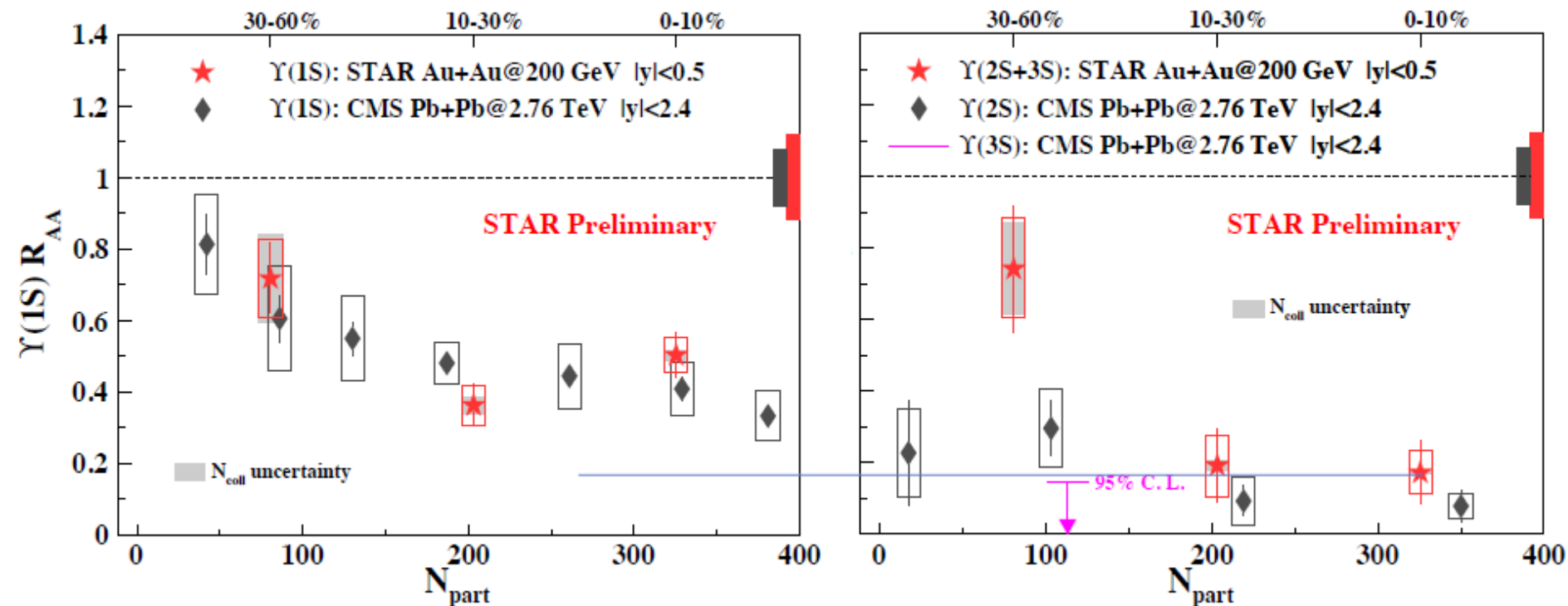
First measurement of centrality dependence of Λ_c production in heavy ion collisions

- Λ_c/D^0 ratio increases from peripheral to central, indicative of hot medium effects
- Ratio for peripheral Au+Au consistent with p+p value at 7 TeV
- Enhancement predicted from coalescence hadronization

Y suppression at 200 GeV



Combined results from $Y \rightarrow e+e-$ and $Y \rightarrow \mu+\mu-$ improve precision of Y measurements



CMS PLB 04, 031 (2017)

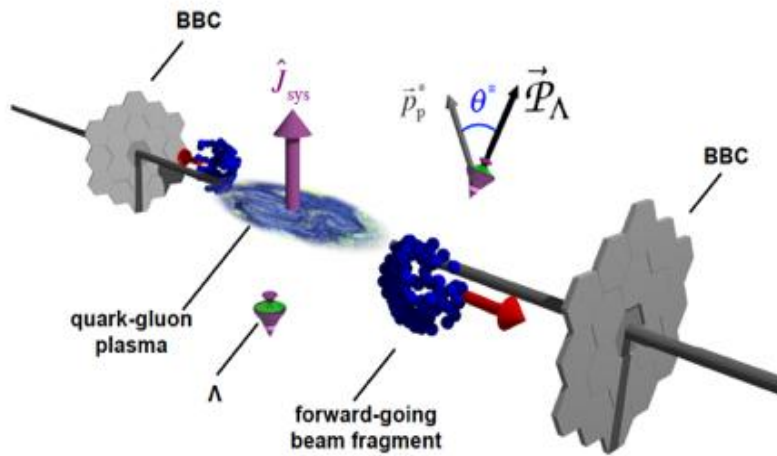
Y(1S) suppression: similar at RHIC and LHC energies!

Y(2S+3S) is more suppressed than Y(1S) in the most central events

$$Y(1S) R_{AA}: 0.50 \pm 0.06 \text{ (stat.)} \pm 0.05 \text{ (sys.)}$$

$$Y(2S+3S) R_{AA}: 0.17 \pm 0.09 \text{ (stat.)} \pm 0.06 \text{ (sys.)}$$

Global Λ polarization



$$\frac{dN}{d \cos \theta^*} = \frac{1}{2} \left(1 + \alpha_H |P_H| \cos \theta^* \right)$$

P_H : Λ /anti- Λ polarization vector in the hyperon rest frame (H denotes Λ /anti- Λ)

α_H : decay parameter $\alpha_\Lambda = -\alpha_{\bar{\Lambda}} = 0.642 \pm 0.013$

Average vorticity points towards the direction of the angular momentum J_{sys} of the collision

Average projection of the polarization on J_{sys} is extracted:

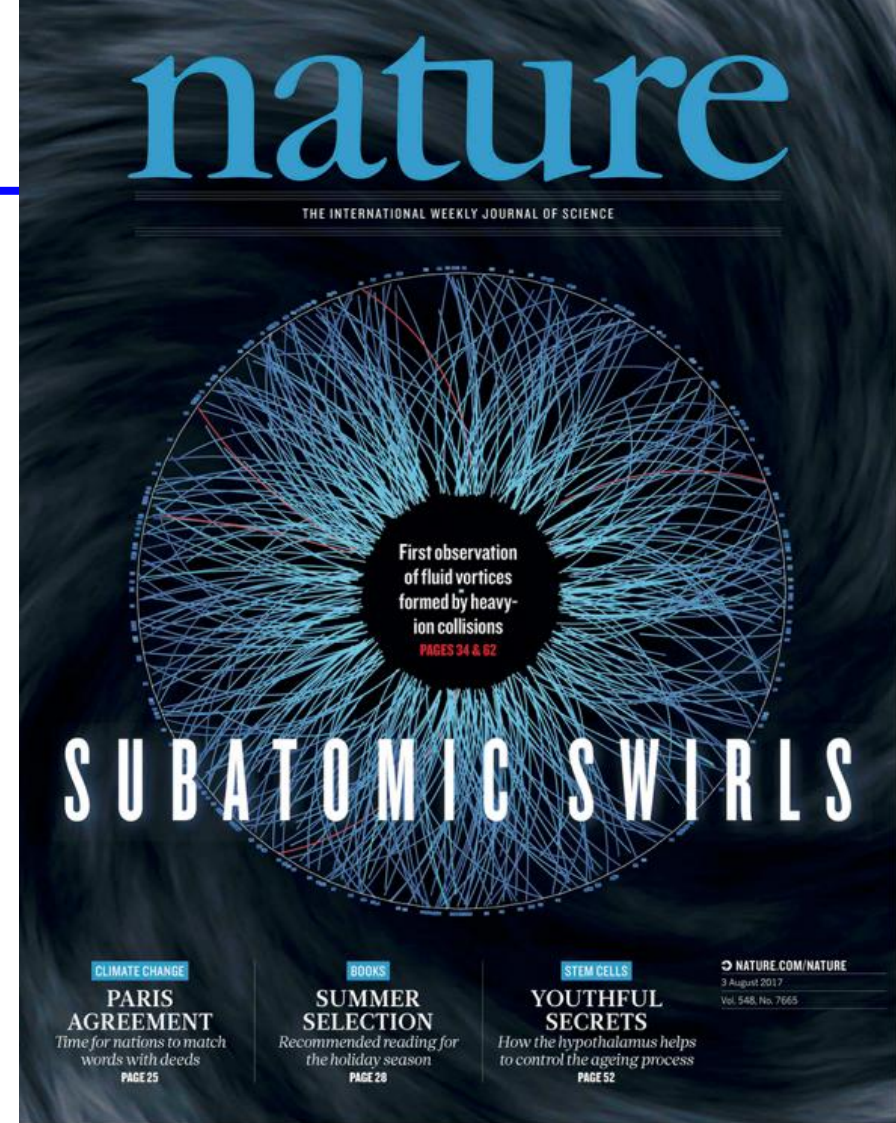
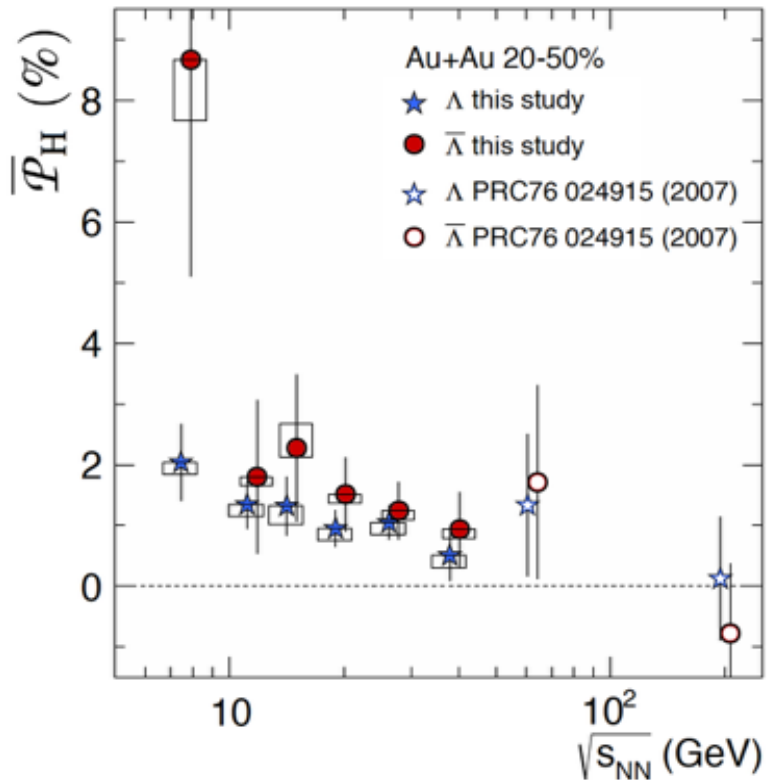
$$\bar{P}_H \equiv \left\langle \vec{P}_H \hat{J}_{sys} \right\rangle = \frac{8}{\pi \alpha_H} \frac{\left\langle \cos(\phi_p^* - \phi_{\hat{J}_{sys}}) \right\rangle}{R_{EP}^1}$$

noted here as global polarization

Global Λ polarization

STAR, Nature, 2017, 1701.06657

First observations of Lambda global polarization

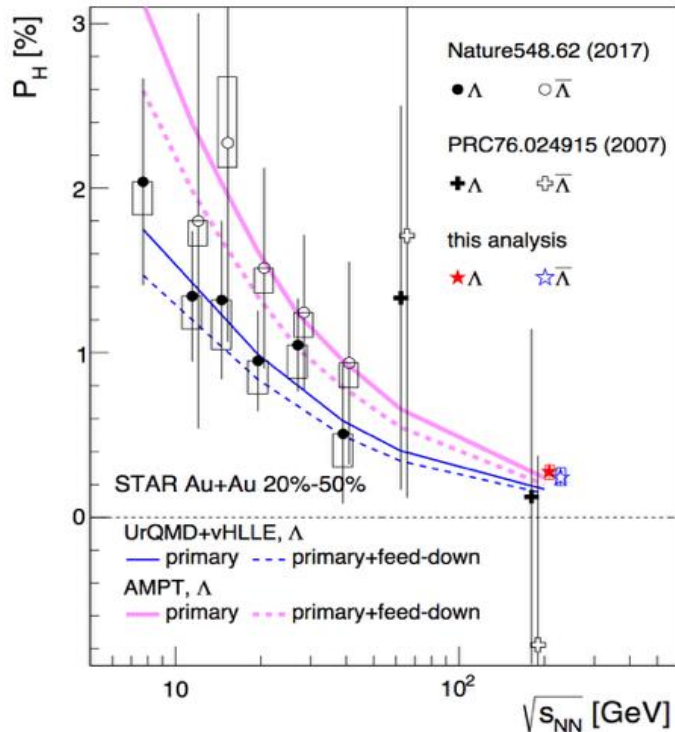


The most vortical fluid

$$\omega = k_B T (\overline{P}_\Lambda + \overline{P}_{\bar{\Lambda}}) / \hbar = 10^{22} s^{-1}$$

Global Λ polarization

Phys. Rev. C 98 (2018) 014910



Data on polarization from 2010, 2011, 2014

Measurements in Au-Au 200 GeV collisions 20-50 % centrality

$$P_H(\Lambda) [\%] = 0.277 \pm 0.040(\text{stat}) \pm_{0.049}^{0.039}(\text{sys})$$

$$P_H(\bar{\Lambda}) [\%] = 0.240 \pm 0.045(\text{stat}) \pm_{0.045}^{0.061}(\text{sys})$$

5-7 σ significance, comparable with BES-I results

No significant difference between Λ and anti- Λ polarization at $\sqrt{s_{\text{NN}}} = 200$ GeV within the uncertainties.

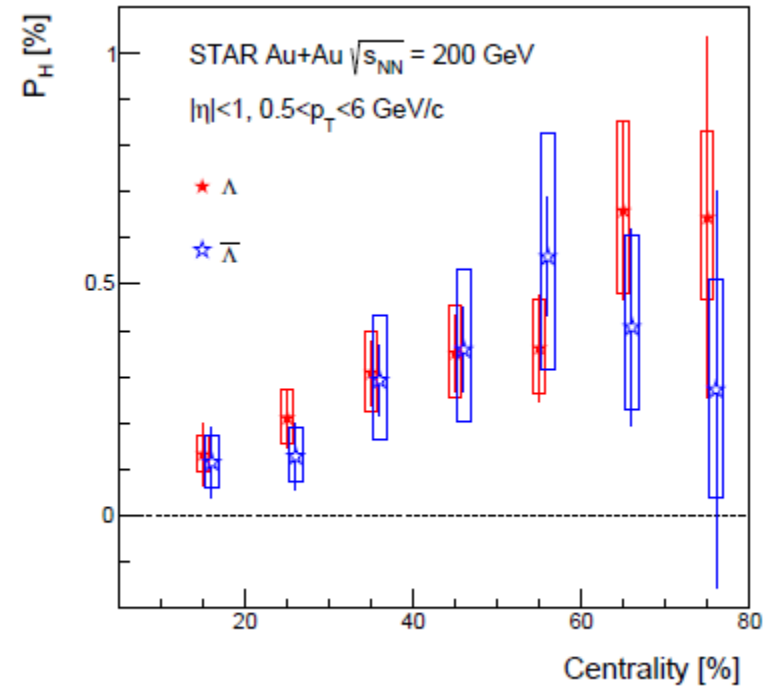
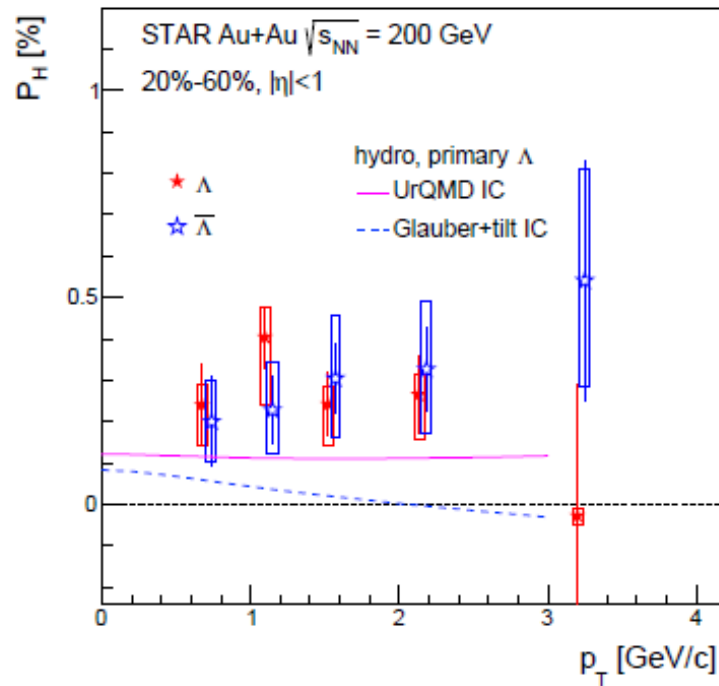
Within the uncertainties these results agree with predictions from a hydrodynamic model (UrQMD+vHILLE) and the AMPT (A Multi-Phase Transport) model.

UrQMD+vHILLE: I. Karpenko and F. Becattini, EPJC (2017)77:213

AMPT: H. Li et al., Phys. Rev. C 96, 054908 (2017)

Polarization dependence on P_T and centrality

Phys. Rev. C 98 (2018) 014910



The polarization was also studied as function of the collision centrality, the hyperon's transverse momentum, and pseudorapidity.

No significant dependence on centrality or transverse momentum was observed.

I. Karpenko and F. Becattini PRL 120.012302, (2018)

Single- and two- particle distributions:

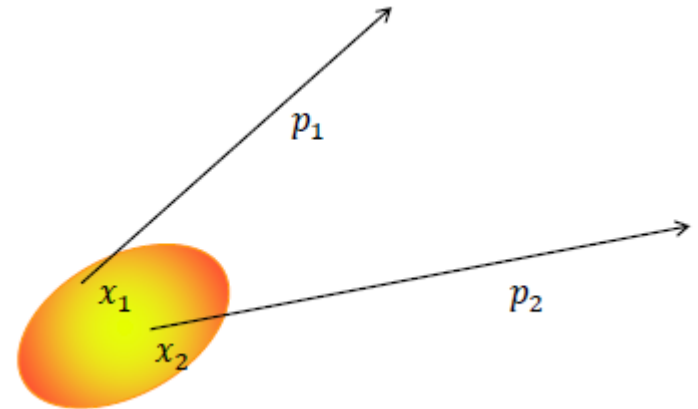
$$P_1(p) = E \frac{dN}{d^3 p} = \int d^4 x S(x, p)$$

$S(x, p)$ – emission function: the distribution of source density probability of finding particle with given x and p

$$P_2(p_1, p_2) = E_1 E_2 \frac{dN}{d^3 p_1 d^3 p_2} = \int d^4 x_1 S(x_1, p_1) d^4 x_2 S(x_2, p_2) \Phi_2(x_2, p_2 / x_1, p_1)$$

Correlation function

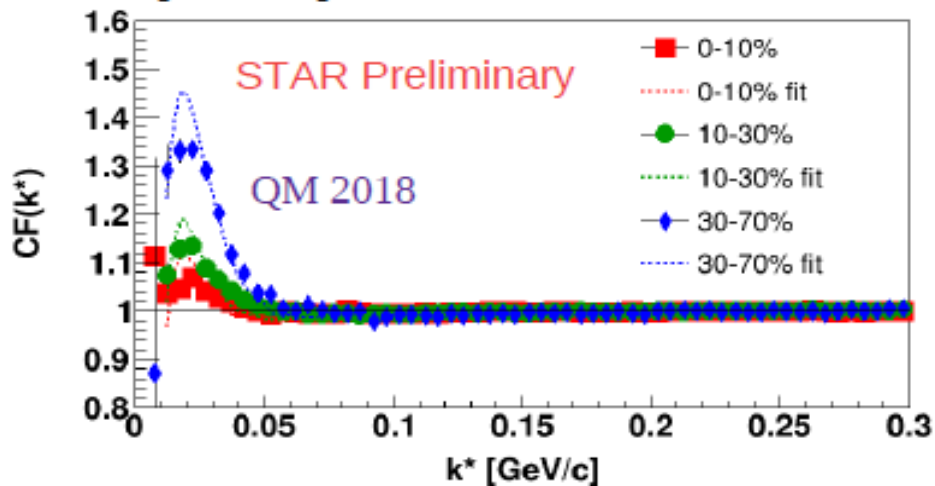
$$C(p_1, p_2) = \frac{P_2(p_1, p_2)}{P_1(p_1) P_1(p_2)}$$



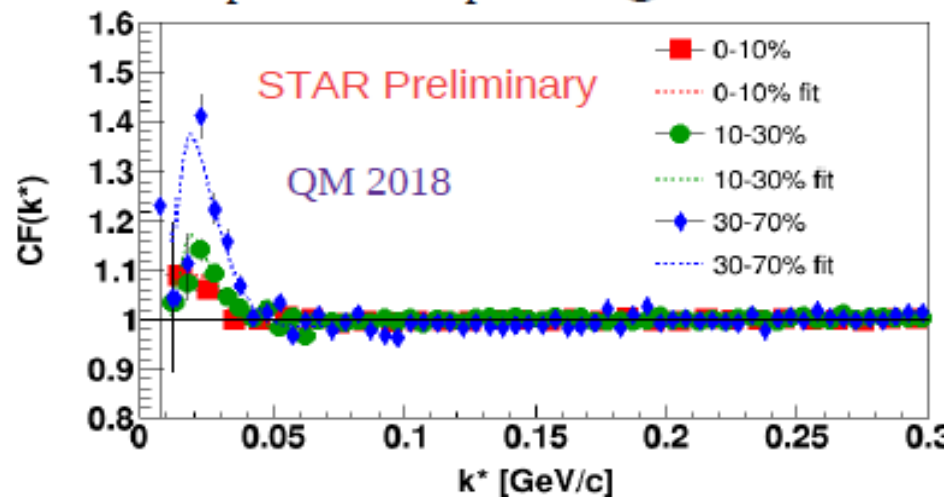
PP correlations



proton-proton @39 GeV



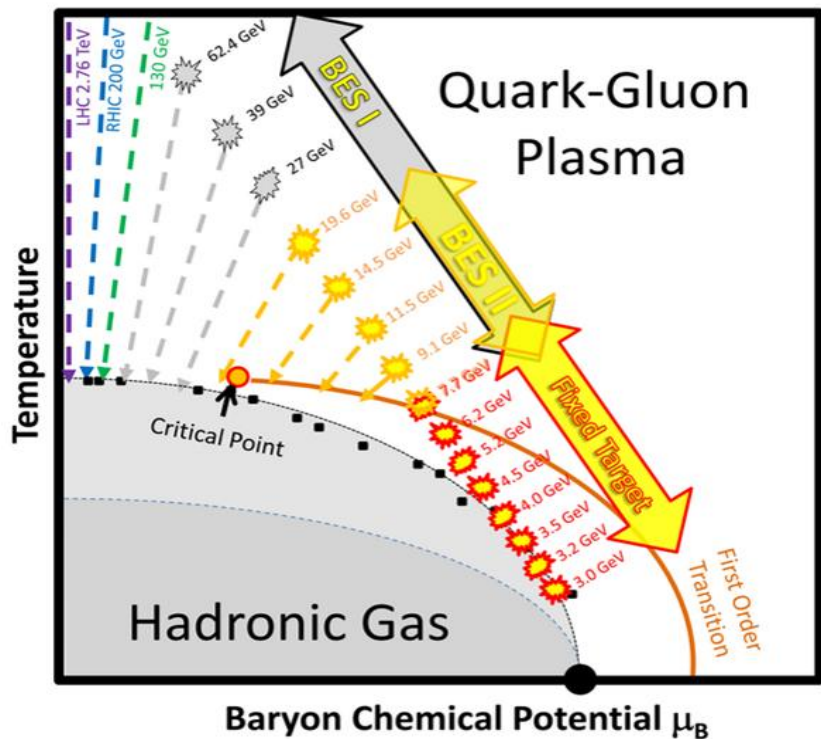
antiproton-antiproton @39 GeV



centrality	$R_{inv} p - p$ [fm]	$R_{inv} \bar{p} - \bar{p}$ [fm]	$R_{inv} p - \bar{p}$ [fm]
0-10%	$4.00 \pm 0.15 \pm 0.02$	$3.83 \pm 0.20 \pm 0.03$	$3.39 \pm 0.12 \pm 0.14$
10-30%	$3.61 \pm 0.13 \pm 0.17$	$3.68 \pm 0.15 \pm 0.11$	$2.69 \pm 0.10 \pm 0.12$
30-70%	$2.72 \pm 0.07 \pm 0.07$	$2.95 \pm 0.11 \pm 0.08$	$2.56 \pm 0.09 \pm 0.12$

- R_{inv} smaller for less central collisions as expected
- No significant difference between p p and p-bar p-bar correlation functions
- Systematically $R_{inv} (p\text{-bar } p) < R_{inv} (p p, p\text{-bar } p\text{-bar})$ which indicates a need to refine low energy p-bar p measurements

Fixed target program at STAR



BES-I main goals:

- Search for 1st order phase transition
- Search for existence of the Critical Point
- Search for turn-off of QGP signatures
- Finished** data taking

Originally BES-I program planned to go down to $v_{NN} = 5$ GeV

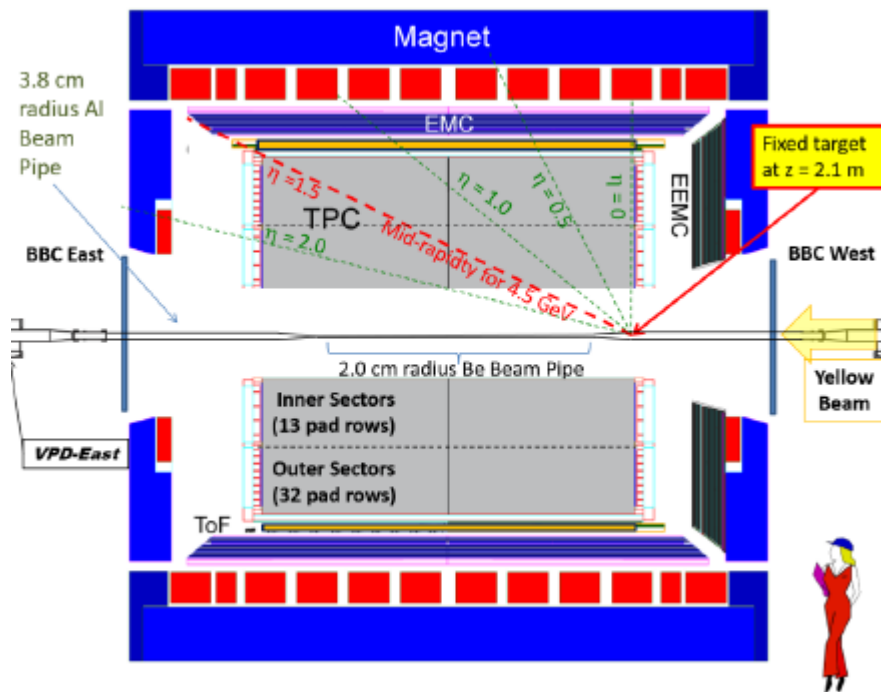
Collider mode

Can not cover energy region $v_{NN} < 7.7$ GeV

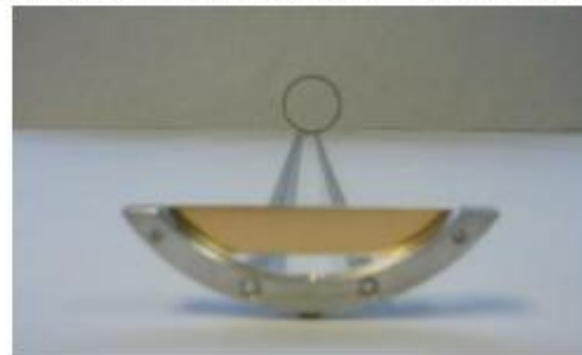
Fixed target mode

Can cover energy region $3 \text{ GeV} < v_{NN} < 7.7 \text{ GeV}$

Fixed target program at STAR



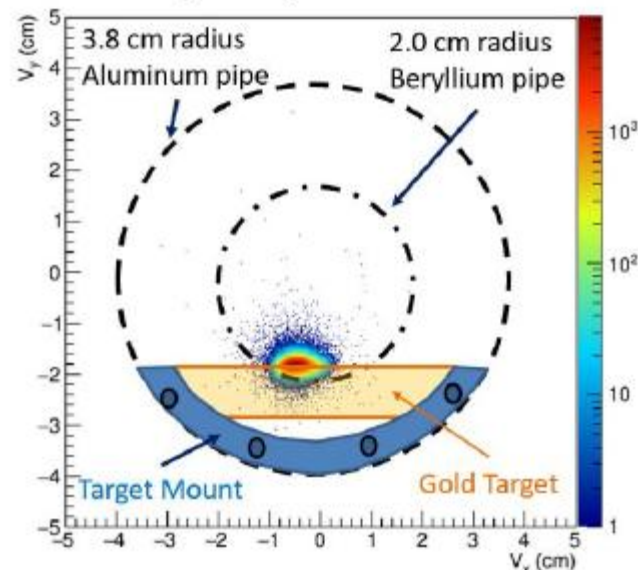
A 1 mm thick (4% inter. prob.) gold target



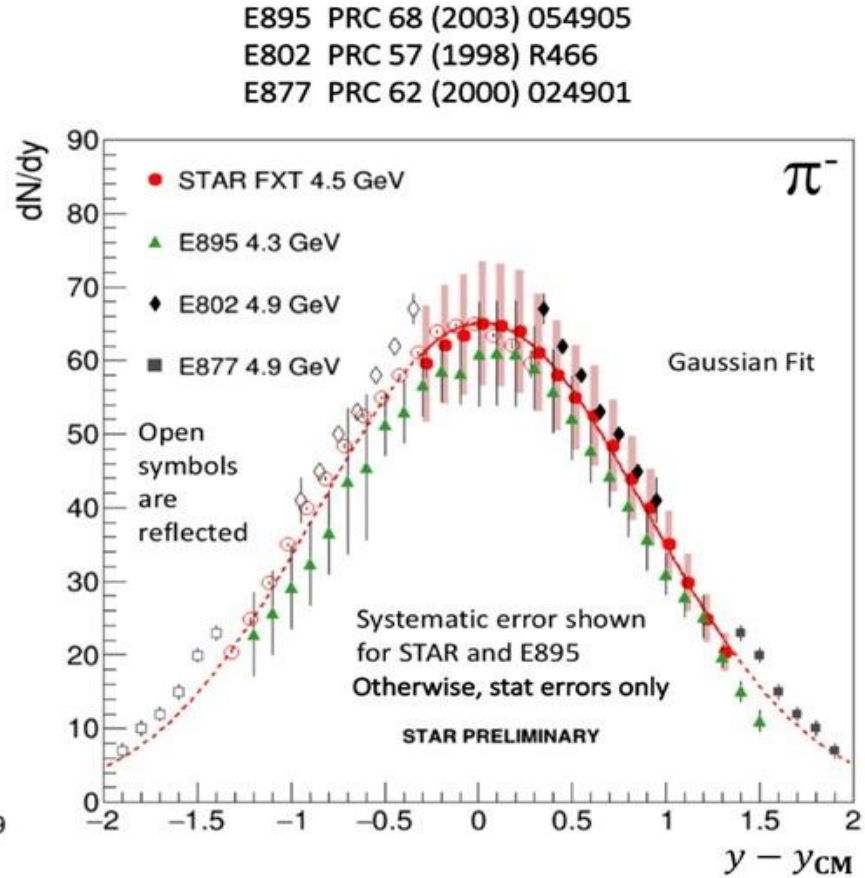
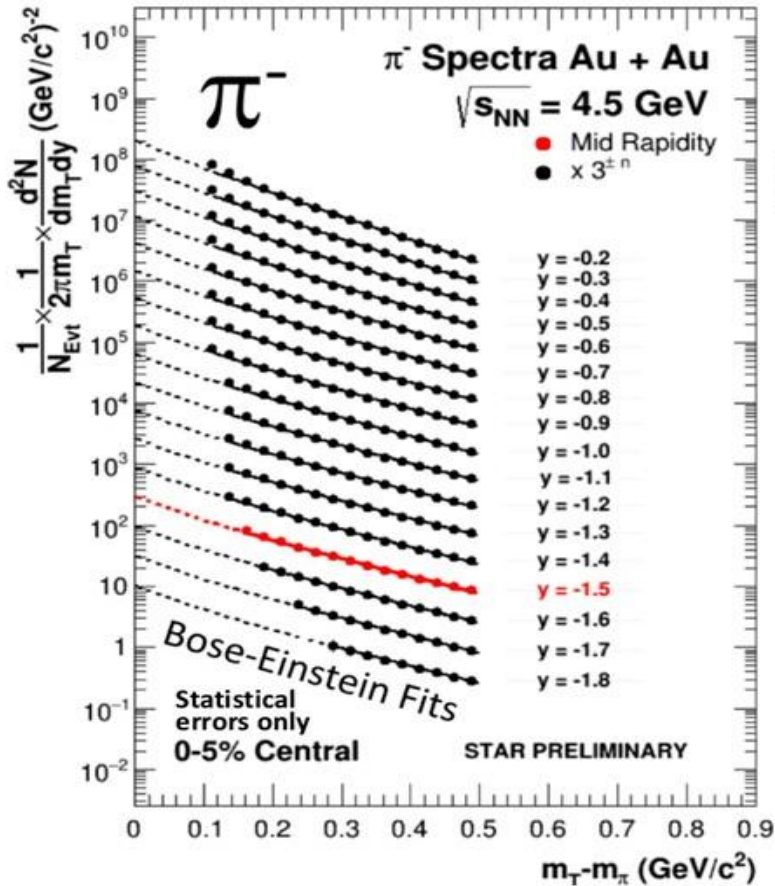
BES Phase II to probe phase diagram of QCD matter, lowest energy is $\sqrt{s_{NN}} = 3$ GeV and cover region lack of experimental data.

BES-II can extend μ_B range from 400 MeV to about 720 MeV

V_y vs. V_x Distribution

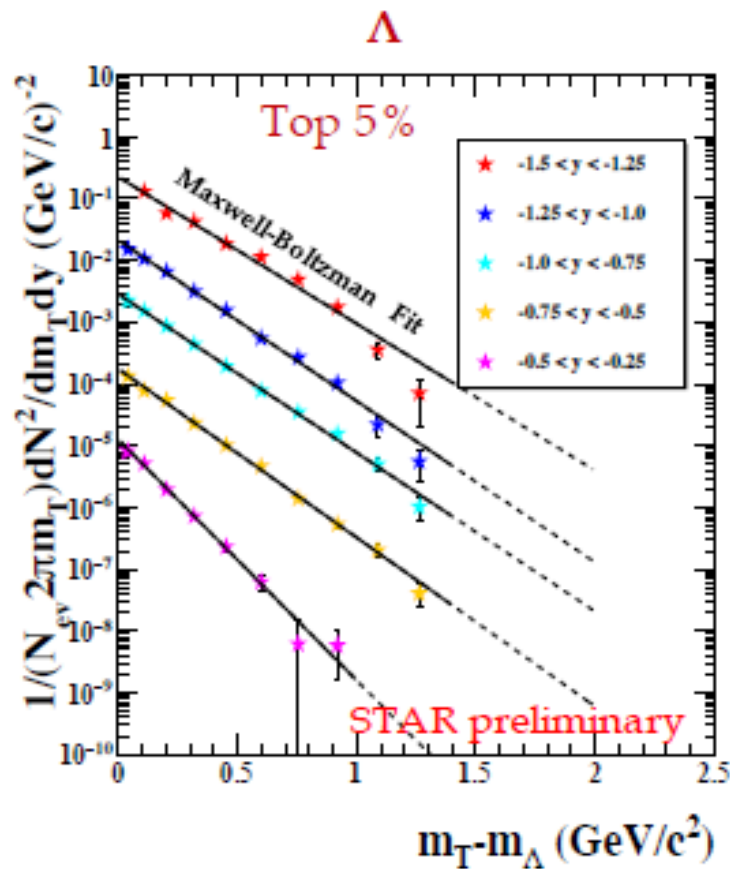
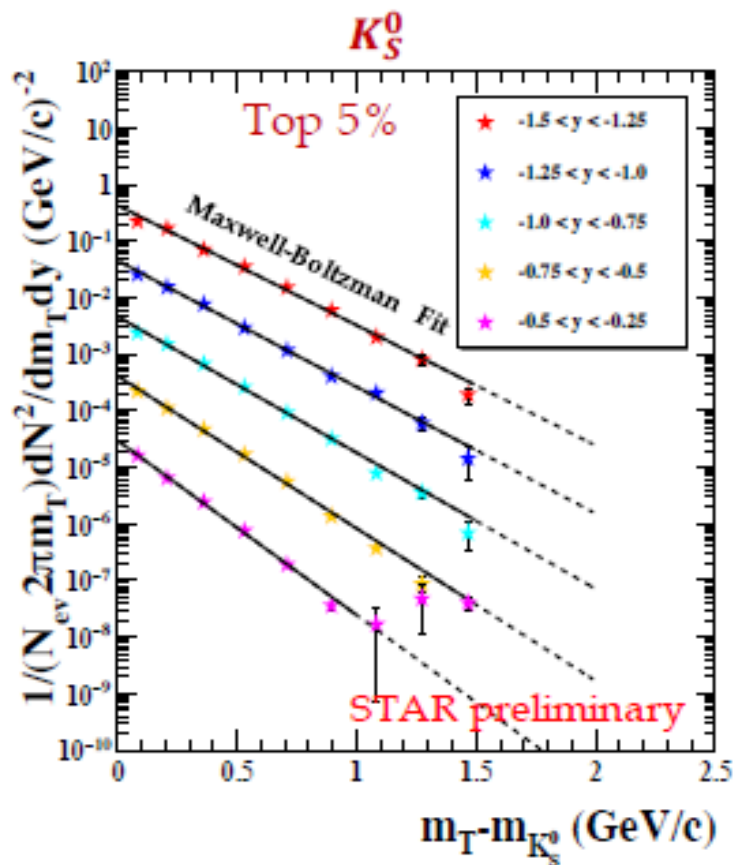


Spectra of π^- in Au-Au at 4.5 GeV FXT



Spectra consistent with AGS results

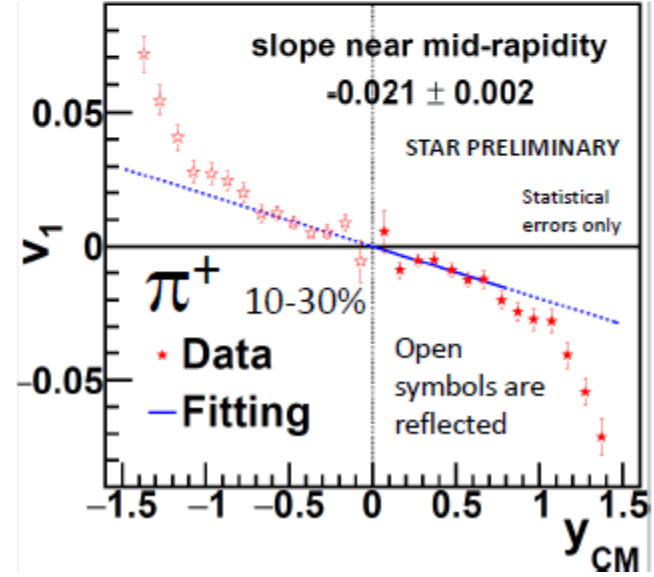
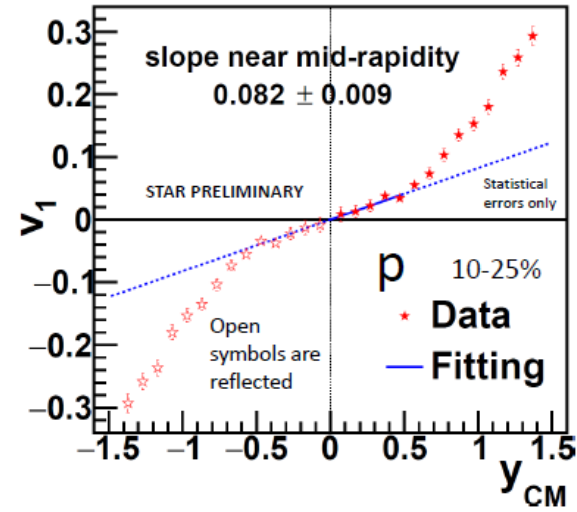
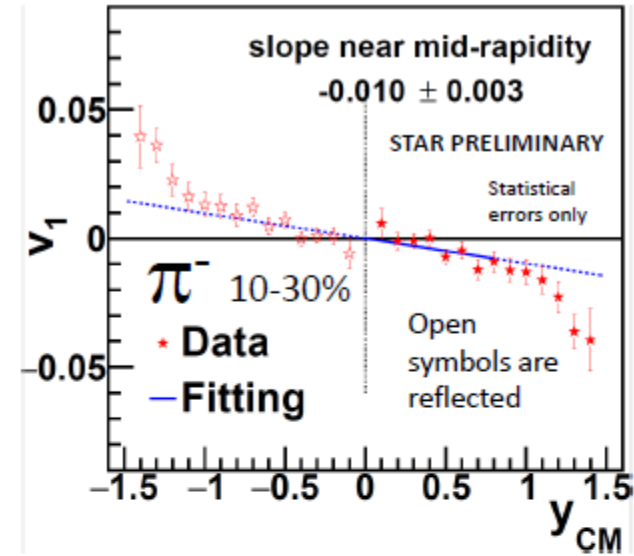
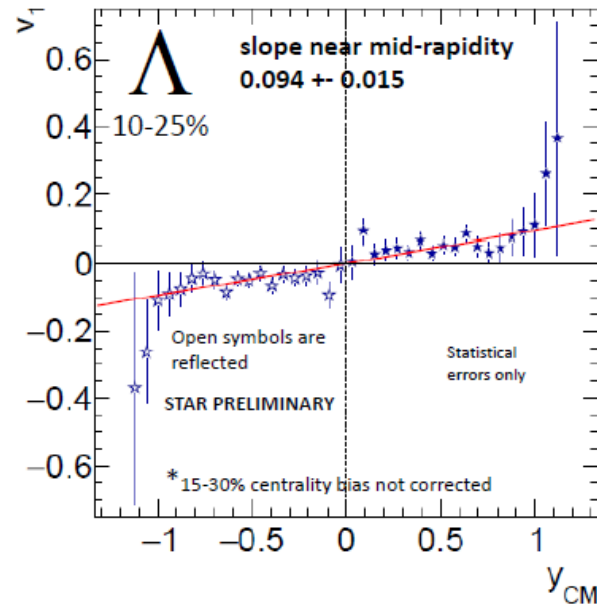
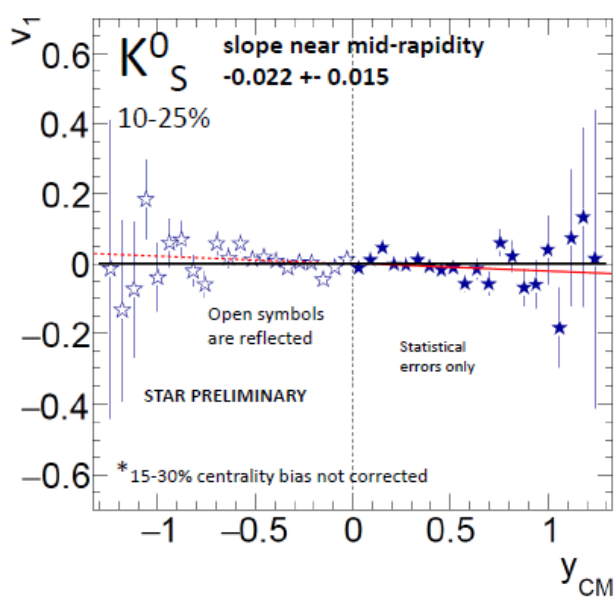
Spectra of K_S^0 and Λ in Au-Au at 4.5 GeV FXT



Statistical errors only

Spectra consistent with AGS results

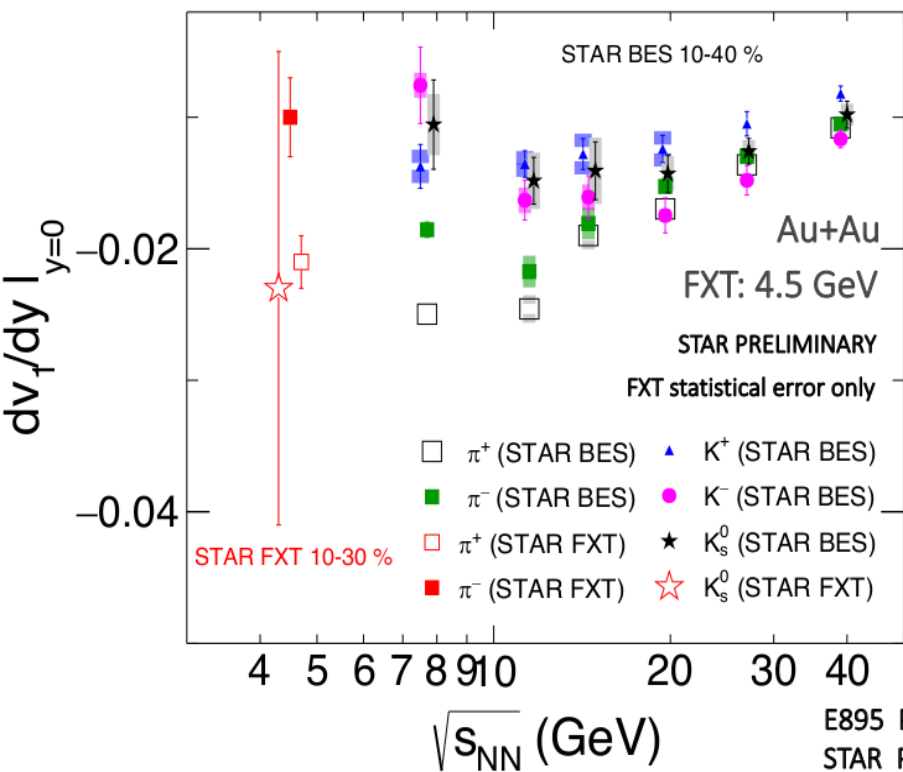
Directed flow v_1 in Au-Au at 4.5 GeV



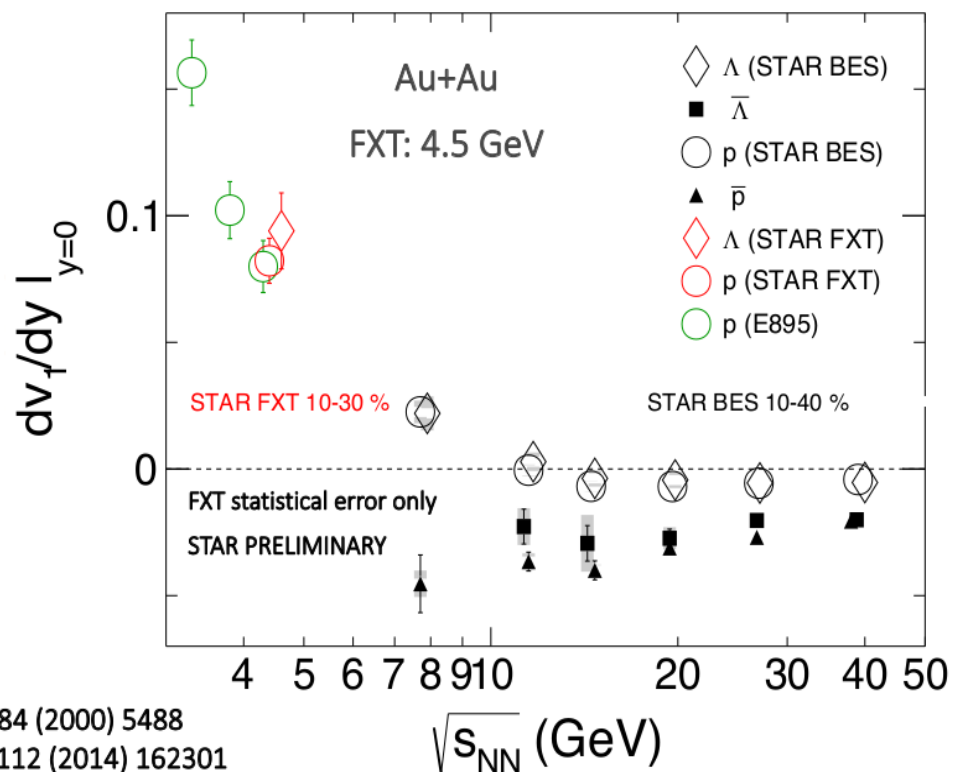
mesons
 pion flow is “negative”
 kaon needs more statistics

baryons
 proton flow is “positive”
 lambda flow is “positive”

Directed flow v_1 energy dependence

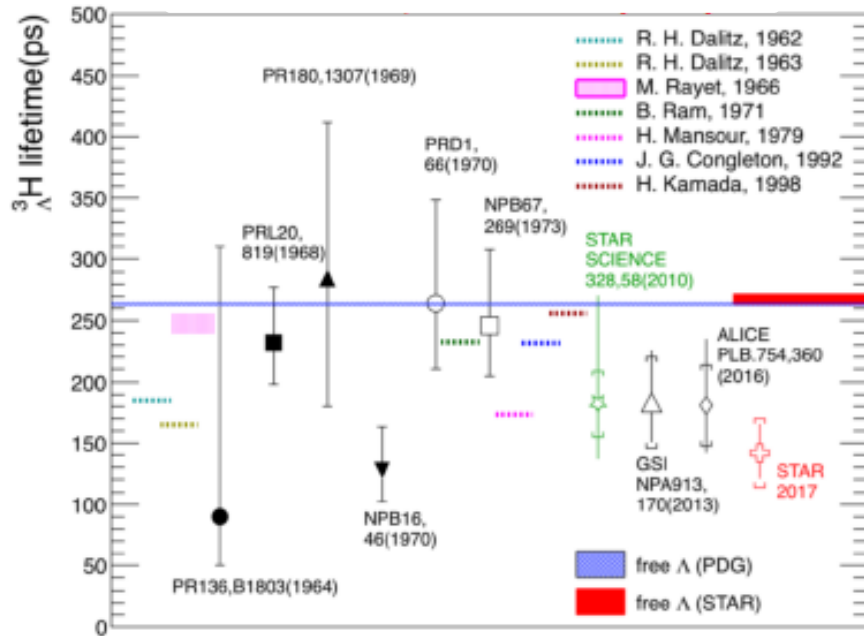


E895 PRL 84 (2000) 5488
STAR PRL 112 (2014) 162301



Proton v_1 agrees with E895; Λ is close to proton

Hypertriton lifetime



Hyperon-Nucleon interactions play an important role in theory of neutron stars and QCD

- measurements of masses of hypertriton and anti-hypertriton provide insight into H-N interactions and the CPT symmetry

- measurements sensitive to the temperature and nucleon phase-space of the system freezout

[1] R. O. Gomes, V. Dexheimer, S. Schramm, and C. A. Z. Vasconcellos, *The Astrophys. J.* 808, 8 (2015).

[2] L. L. Lopes and D. P. Menezes, *Phys. Rev. C* 89, 025805 (2014).

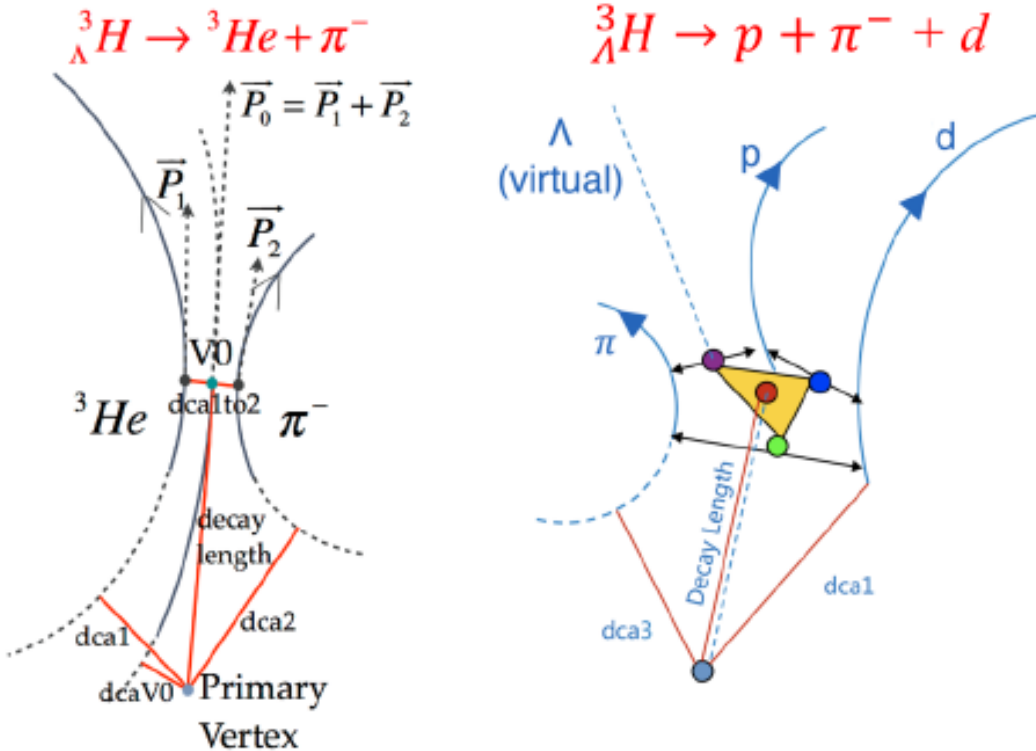
[3] J. Antoniadis et al., *Science* 340, 448 (2013).

[4] László P. Csernai, Joseph I. Kapusta, *Phys. Repts.* 131, 223 (1986).

[5] A. Z. Meljjan, *Phys. Rev. C* 17, 1051 (1978).

[6] Kaijia Sun et al., *Phys. Lett. B* 774, 103 (2017).

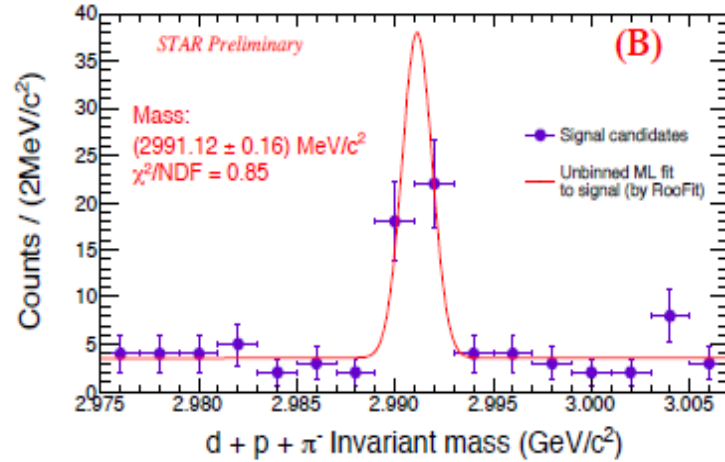
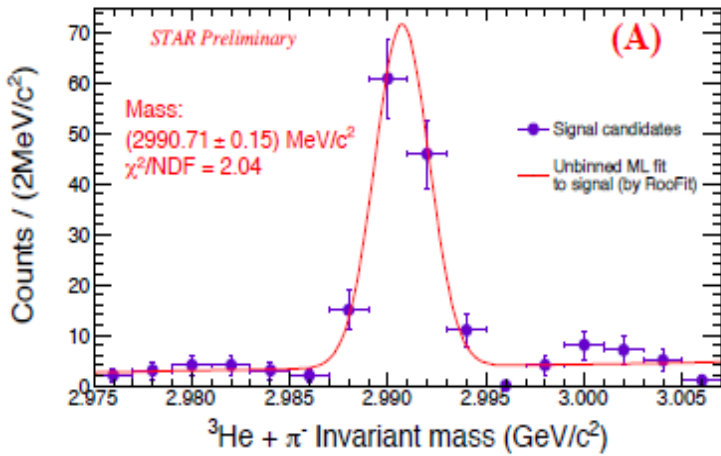
Hypertriton reconstruction with HFT



- ${}^3_{\Lambda}H$ has many decay channels:
- ✓ Non-meson decay channels:
 - ${}^3_{\Lambda}H \rightarrow d + n$
 - ${}^3_{\Lambda}H \rightarrow p + n + n$
 - ✓ Meson decay channels:
 - ${}^3_{\Lambda}H \rightarrow {}^3He$ (3H) + π^- (π^0)
 - ${}^3_{\Lambda}H \rightarrow d + p$ (n) + π^- (π^0)
 - ${}^3_{\Lambda}H \rightarrow p + n + p$ (n) + π^- (π^0)
- Good PID of charged particles in STAR detector.**
- Reconstructing ${}^3_{\Lambda}H$ (${}^3_{\Lambda}\bar{H}$) through:**
- ${}^3_{\Lambda}H \rightarrow {}^3He + \pi^-$
 - ${}^3_{\Lambda}H \rightarrow d + p + \pi^-$

High spatial resolution of HFT (< 30 μm) allows precise determination of the decay vertex

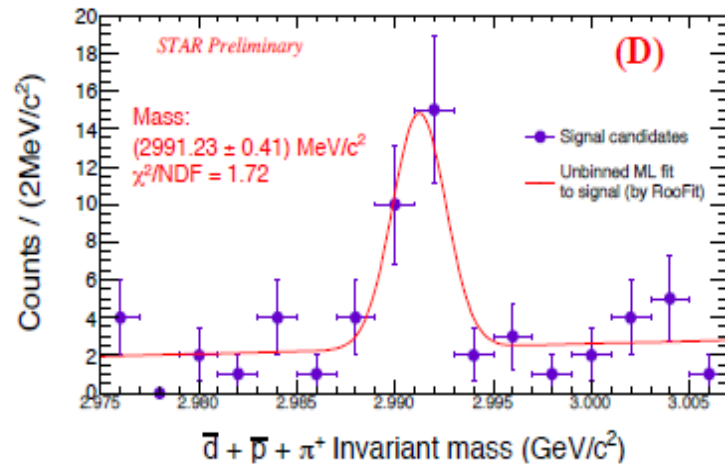
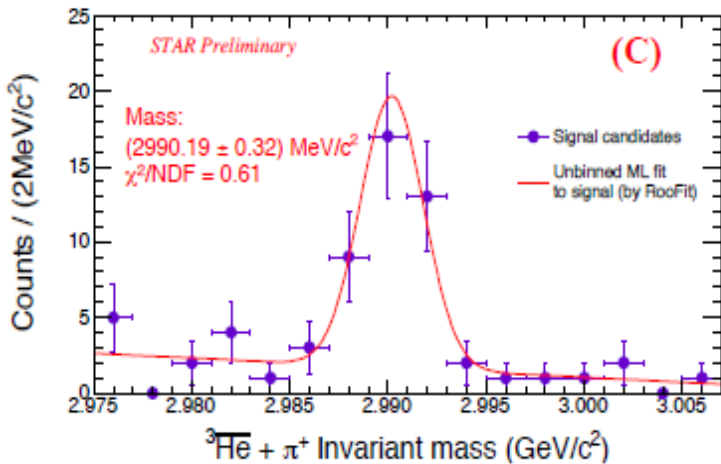
$\Lambda^3\text{H}$ and anti- $\Lambda^3\text{H}$ mass reconstruction



$\Lambda^3\text{H}$ (2-body + 3-body)
2990.90 ± 0.11 (stat.) ± 0.15 (syst.) MeV/c²

$\bar{\Lambda}^3\text{H}$ (2-body + 3-body)
2990.59 ± 0.25 (stat.) ± 0.15 (syst.) MeV/c²

$\Lambda^3\text{H}$ and $\bar{\Lambda}^3\text{H}$ combined
2990.85 ± 0.10 (stat.) ± 0.15 (syst.) MeV/c²



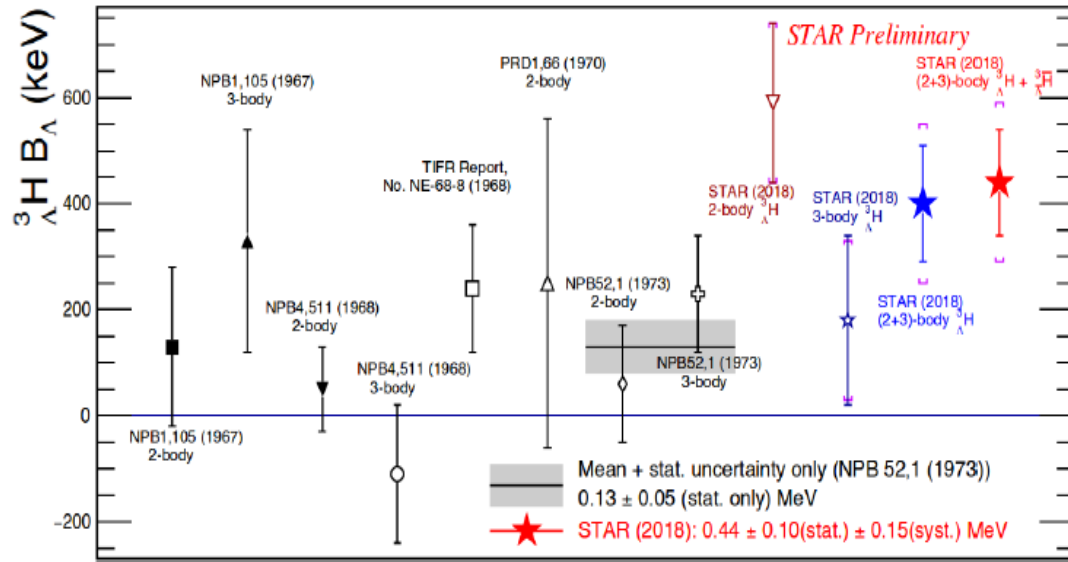
Systematical uncertainty source:
 > Energy loss correction.
 > Different cuts impact.

Fit Function:

$$N_{\text{sig}} \left(\frac{1}{\sqrt{2\pi\sigma^2}} e^{-\frac{(x-\mu)^2}{2\sigma^2}} \right) + N_{\text{bkg}}(ax + b)$$

Energy loss corrections applied

Hypertriton and CPT symmetry



Hypertriton binding energy definition:

$$m_{\Lambda} + m_d - m_{\Lambda^3\text{H}} = 0.44 \pm 0.10(\text{stat.}) \pm 0.15(\text{syst.})\text{MeV}$$

Mass difference between $\Lambda^3\text{H}$ and anti- $\Lambda^3\text{H}$ was measured for the first time

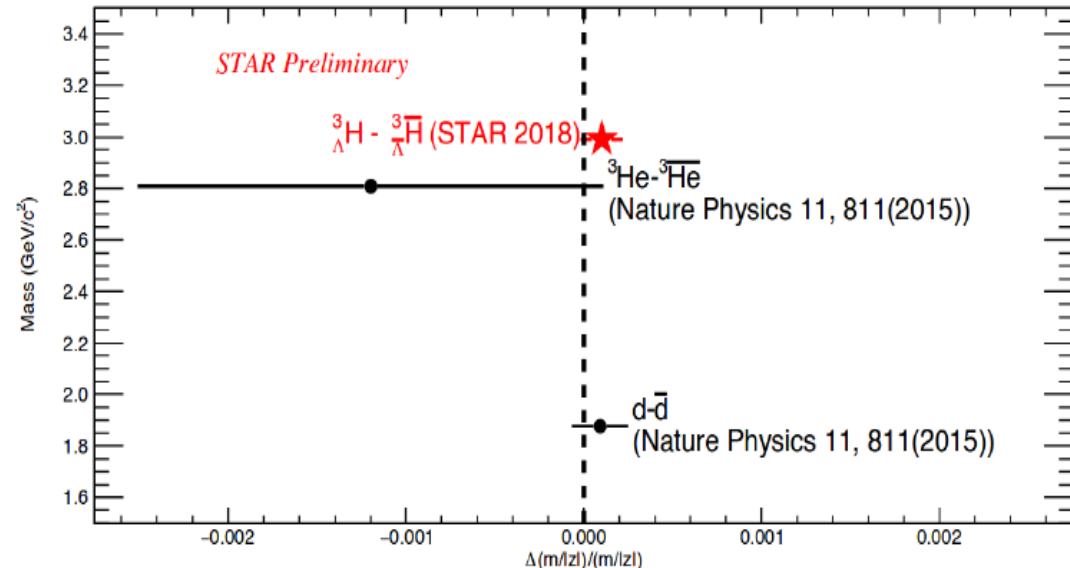
First test of CPT symmetry in light hypernuclei sector.

Mass difference is zero within the uncertainties.

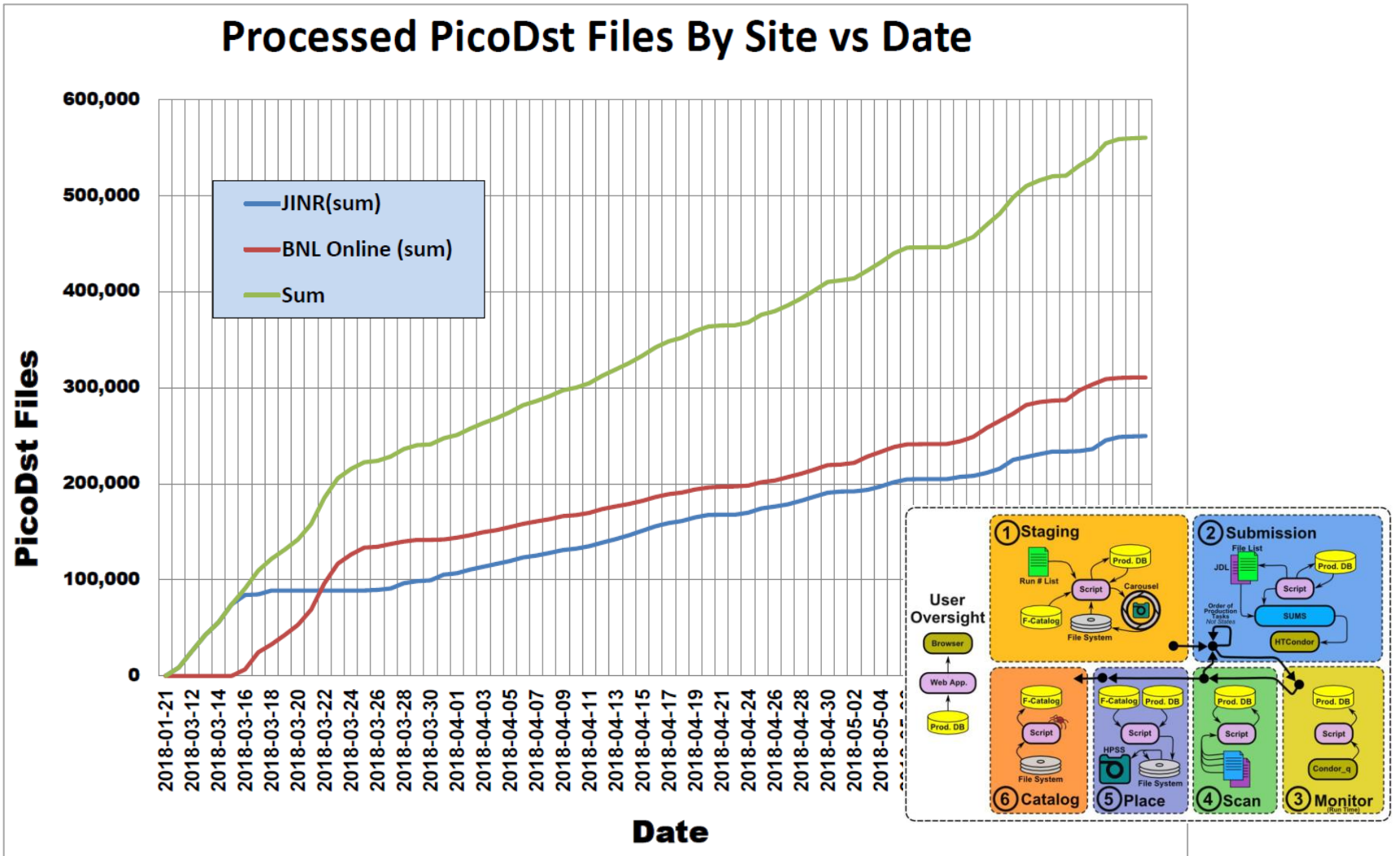
$$\left(\frac{\Delta(m/|z|)}{m/|z|} \right)_d = (0.9 \pm 0.5(\text{stat.}) \pm 1.4(\text{syst.})) \times 10^{-4}$$

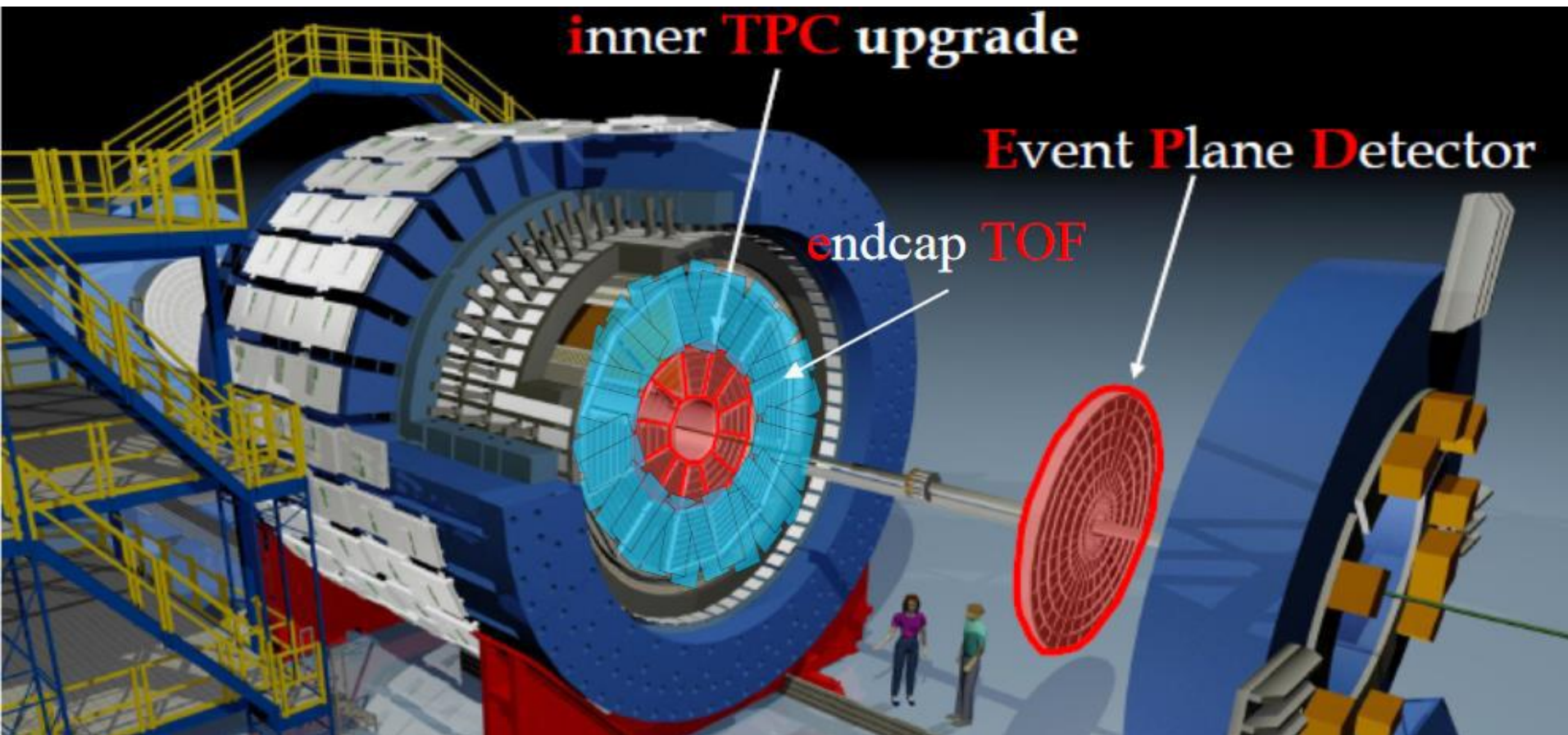
$$\left(\frac{\Delta(m/|z|)}{m/|z|} \right)_{^3\text{He}} = (-1.2 \pm 0.9(\text{stat.}) \pm 1.0(\text{syst.})) \times 10^{-3}$$

$$\left(\frac{\Delta m}{m} \right)_{\Lambda^3\text{H}} = (1.0 \pm 0.9(\text{stat.}) \pm 0.7(\text{syst.})) \times 10^{-4}$$



Transfer of production data to PicoDST





inner TPC upgrade

Event Plane Detector

endcap TOF

EPD installed

- $2.1 < |\eta| < 5.1$
- Improves EP resolution
- Independent trigger

iTPC upgrade 2019

- $p_T > 60$ MeV/c
- $|\eta| < 1.5$
- Improvement of dE/dx resolution

eTOF upgrade 2019

- $-1.6 < \eta < -1.1$
- Extends forward PID capability

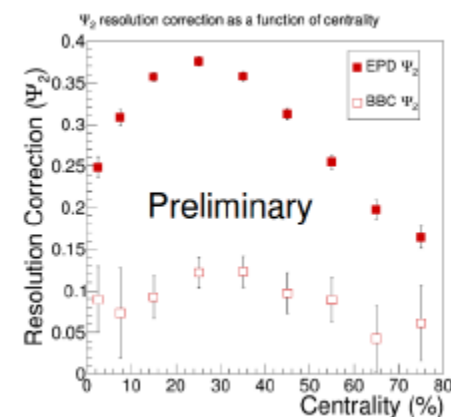
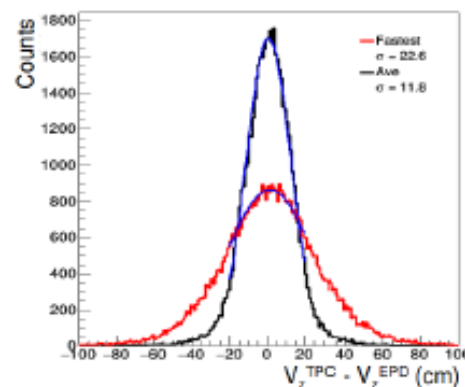
Event Plane Detector



- ✓ **2 wheels**
 - East and West EPD ($2.1 < |\eta| < 5.1$)
- ✓ **12 supersectors**
 - Scintillator wedges, milled to form 31 tiles
 - Optically separated by epoxy
- ✓ **Fiber optics**
 - Wavelength shifting fibers
- ✓ **Sensors**
 - Silicon Photon Multipliers (SiMP)



- All 744 tiles are good
- Timing resolution about 0.75 ns with fastest TAC method
- The 2nd order event plane resolution is 0.37 in 20-30% central events in isobar collisions



STAR Note 0666: An Event Plane Detector for STAR

✓ Inner sectors

- Increase readout pad rows (13 to 40)
- New wire frames
- New designed strongback

✓ New electronics for inner sectors

- Doubled readout channels. Use ALICE SAMPA chip

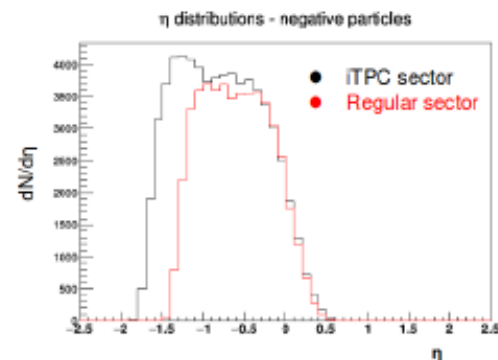
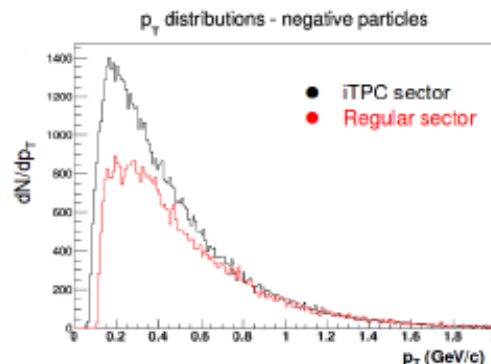
✓ New designed insertion tooling

✓ Replace all 24 inner sectors

- One sector has been installed and used in the data taking 2018
- Full installation in fall 2018



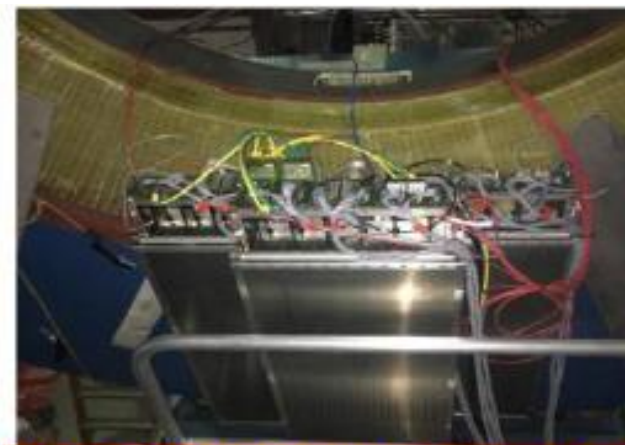
- Maximum hits per track 45 -> 72
- Lower transverse momentum threshold of 60 MeV/c
- Extends $|\eta|$ coverage 1.1 -> 1.5



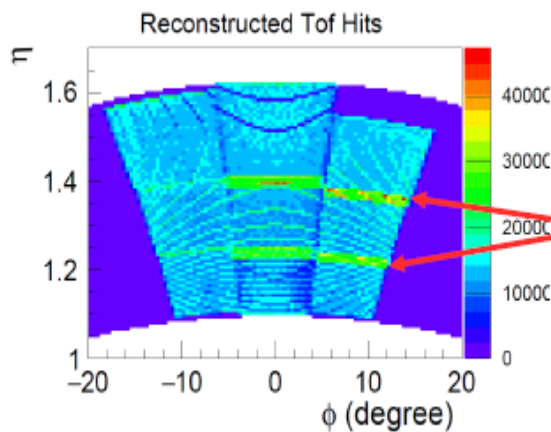
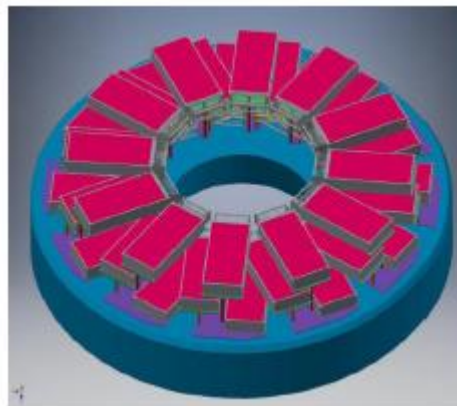
eTOF upgrade



- ✓ Install, commission and use 10% of the CBM TOF modules in STAR
- ✓ Design concept
 - 3 layers, 12 sectors, 36 modules, 108 MRPCs
- ✓ PID in the forward direction
- ✓ One sector with three modules has been installed and used in the data taking 2018
- ✓ Full installation in fall 2018

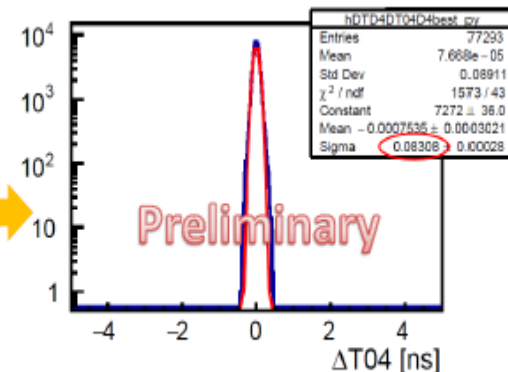


3 eTOF modules have been installed



Overlap range of two MRPCs

Time resolution



- ✓ System time resolution: 83 ps
- ✓ Counter time resolution: 59 ps

STAR future program



Collision Energy (GeV)	7.7	9.1	11.5	14.5	19.6
μ_B (MeV) in 0-5% central collisions	420	370	315	260	205
Observables					
R_{CP} up to $p_T = 5$ GeV/c	-		160	125	92
Elliptic Flow (ϕ mesons)	80	120	160	160	320
Chiral Magnetic Effect	50	50	50	50	50
Directed Flow (protons)	20	30	35	45	50
Azimuthal Femtoscopy (protons)	35	40	50	65	80
Net-Proton Kurtosis	70	85	100	170	340
Dileptons	100	160	230	300	400
$>5\sigma$ Magnetic Field Significance	50	80	110	150	200
Required Number of Events	100	160	230	300	400

STAR BES-II and FXT programs will cover broad range of interest

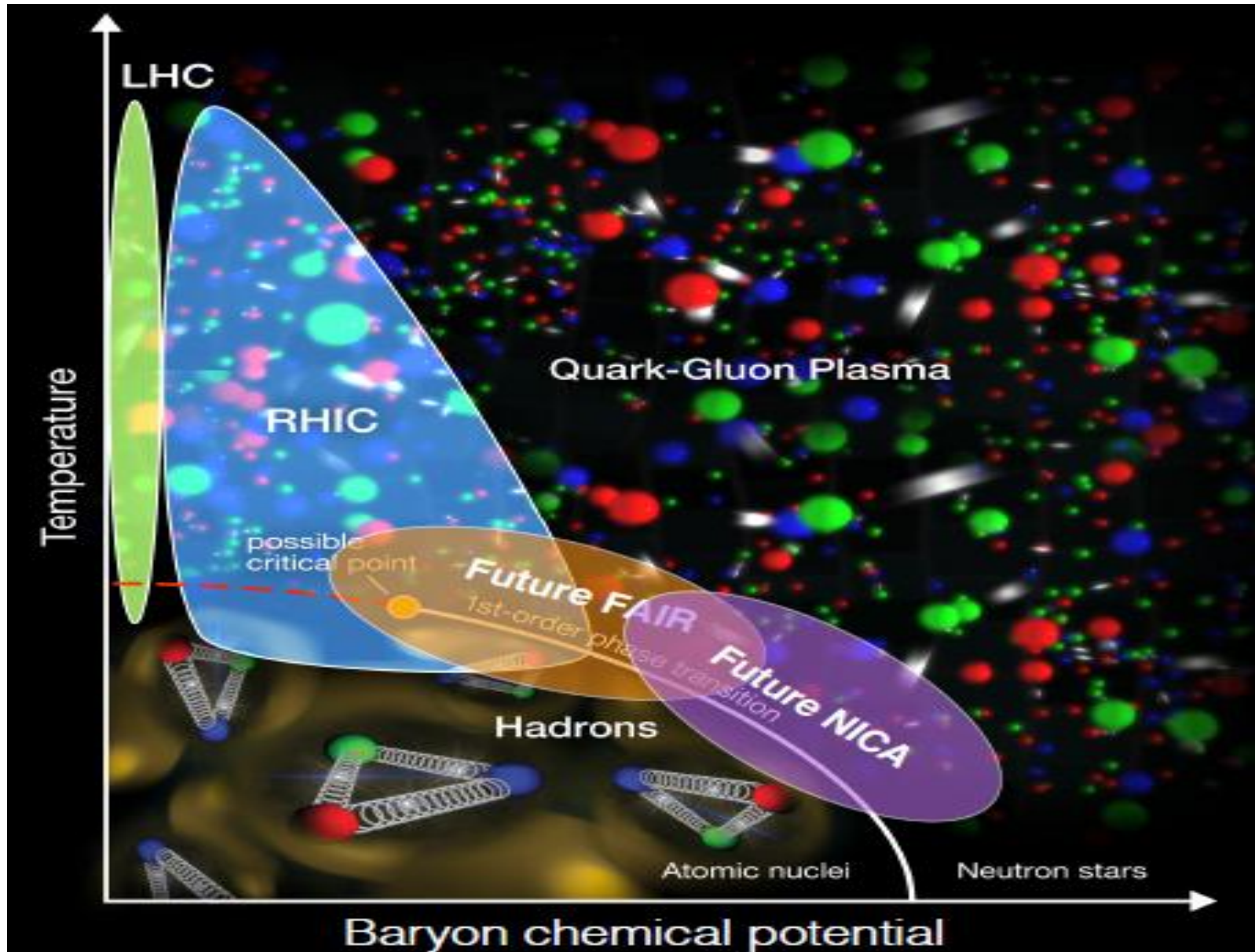
FXT

- Data rate is DAQ limited
- iTPC & eTOF will be available
- Will have an overlap with the collider data for 7.7 GeV

Single Beam Energy (GeV/nucleon)	$\sqrt{s_{NN}}$ (GeV)	Run Year	Run Time	Species	Min-Bias Events Number
5.75	3.5 (FXT)	2020	2 days	Au+Au	100M
7.3	3.9 (FXT)	2019	2 days	Au+Au	100M
9.8	4.5 (FXT)	2019	2 days	Au+Au	100M
13.5	5.2 (FXT)	2020	2 days	Au+Au	100M
19.5	6.2 (FXT)	2020	2 days	Au+Au	100M
31.2	7.7 (FXT)	2019	2 days	Au+Au	100M

STAR Note 0696: Beam Use Request for Run19+

Thank you for the attention!

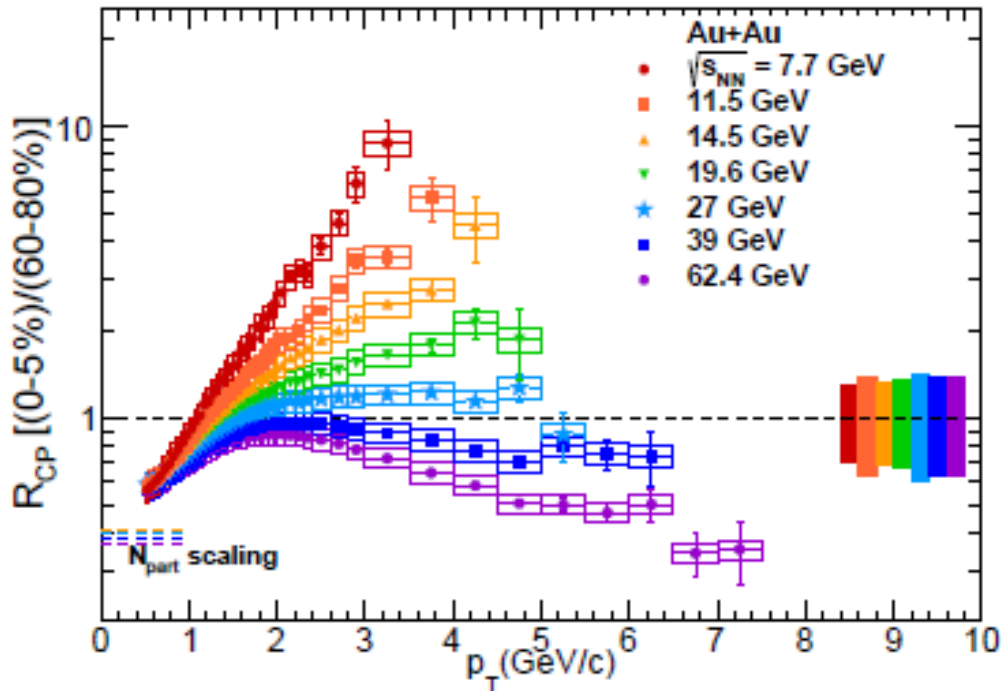




Backup slides

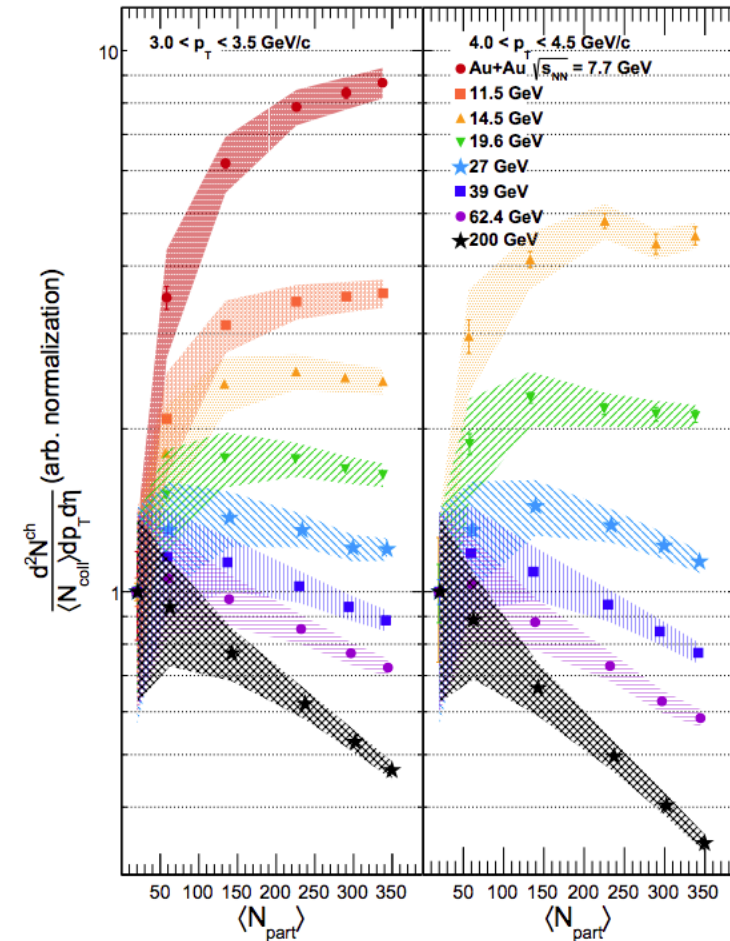
Results from BES-I

$$R_{cp} = \frac{d^2 N dp_t d\eta / \langle N_{bin} \rangle (central)}{d^2 N dp_t d\eta / \langle N_{bin} \rangle (peripheral)}$$



R_{CP} of charged hadrons

- Becomes smaller than 1 at 39 GeV and higher
- Reaches plateau at 19.6 GeV and 27 GeV



Present and future HIC experimental programs

